

1970

# Heat capacities of four rare earth trichloride hexahydrates from 5 to 300°K

Donald Clarence Rulf  
*Iowa State University*

Follow this and additional works at: <https://lib.dr.iastate.edu/rtd>

 Part of the [Physical Chemistry Commons](#)

## Recommended Citation

Rulf, Donald Clarence, "Heat capacities of four rare earth trichloride hexahydrates from 5 to 300°K " (1970). *Retrospective Theses and Dissertations*. 4788.  
<https://lib.dr.iastate.edu/rtd/4788>

This Dissertation is brought to you for free and open access by the Iowa State University Capstones, Theses and Dissertations at Iowa State University Digital Repository. It has been accepted for inclusion in Retrospective Theses and Dissertations by an authorized administrator of Iowa State University Digital Repository. For more information, please contact [digirep@iastate.edu](mailto:digirep@iastate.edu).

71-7321

RULF, Donald Clarence, 1940-  
HEAT CAPACITIES OF FOUR RARE EARTH  
TRICHLORIDE HEXAHYDRATES FROM 5 TO  
300°K.

Iowa State University, Ph.D., 1970  
Chemistry, physical

**University Microfilms, Inc., Ann Arbor, Michigan**

HEAT CAPACITIES OF FOUR RARE EARTH TRICHLORIDE  
HEXAHYDRATES FROM 5 TO 300<sup>0</sup>K

by

Donald Clarence Rulf

A Dissertation Submitted to the  
Graduate Faculty in Partial Fulfillment of  
The Requirements for the Degree of  
DOCTOR OF PHILOSOPHY

Major Subject: Physical Chemistry

Approved:

Signature was redacted for privacy.

In Charge of Major Work

Signature was redacted for privacy.

Head of Major Department

Signature was redacted for privacy.

Dean of Graduate College

Iowa State University  
Ames, Iowa

1970

PLEASE NOTE:

Some pages have indistinct  
print. Filmed as received.

UNIVERSITY MICROFILMS.

## TABLE OF CONTENTS

	Page
I. INTRODUCTION	1
II. LITERATURE SURVEY	4
III. EXPERIMENTAL DETAILS	20
A. Samples	20
B. Apparatus	27
C. Procedures	54
IV. RESULTS	59
A. Heat Capacities	59
B. Magnetic Heat Capacities	83
C. Solution Entropies	95
V. DISCUSSION	102
A. Heat Capacities	102
B. Magnetic Heat Capacities	108
C. Solution Entropies	115
VI. BIBLIOGRAPHY	118
VII. ACKNOWLEDGEMENTS	124

## LIST OF TABLES

Table	Page
1 Results of emission spectroscopic analyses	25
2 Results of mass spectroscopic analyses	26
3 Experimental values of $Q/\Delta T$ for the addenda	60
4 Experimental values of $Q/\Delta T$ for benzoic acid	63
5 Experimental values of $Q/\Delta T$ for $\text{GdCl}_3 \cdot 6\text{H}_2\text{O}$	67
6 Experimental values of $Q/\Delta T$ for $\text{TbCl}_3 \cdot 6\text{H}_2\text{O}$	73
7 Experimental values of $Q/\Delta T$ for $\text{HoCl}_3 \cdot 6\text{H}_2\text{O}$	75
8 Experimental values of $Q/\Delta T$ for $\text{LuCl}_3 \cdot 6\text{H}_2\text{O}$	84
9 Lattice contribution to the thermodynamic functions of $\text{GdCl}_3 \cdot 6\text{H}_2\text{O}$ for $T \leq 14^\circ\text{K}$	86
10 Lattice plus magnetic contributions to the thermodynamic functions of $\text{GdCl}_3 \cdot 6\text{H}_2\text{O}$	87
11 Thermodynamic functions of $\text{TbCl}_3 \cdot 6\text{H}_2\text{O}$	89
12 Thermodynamic functions of $\text{HoCl}_3 \cdot 6\text{H}_2\text{O}$	90
13 Thermodynamic functions of $\text{LuCl}_3 \cdot 6\text{H}_2\text{O}$	92
14 Standard state entropies	101

## LIST OF FIGURES

Figure	Page
1 Vapor pressure as a function of solute concentration for the $\text{RCl}_3 - \text{H}_2\text{O}$ system	23
2 Some of the principal features of the calorimeter	31
3 Details of the calorimeter can, adiabatic shield, and heater/thermometer assembly	35
4 Wiring diagram of the semi-automatic adiabatic shield control system	42
5 Difference function for studying the smoothness of the temperature dependence of the Minco thermometer resistance	47
6 Some of the principal features of the White double potentiometer	51
7 Difference function relating the present and some previously published benzoic acid heat capacities	65
8 Smoothed curve heat capacity of $\text{GdCl}_3 \cdot 6\text{H}_2\text{O}$	71
9 Heat capacity of $\text{HoCl}_3 \cdot 6\text{H}_2\text{O}$ in the temperature region below $20^\circ\text{K}$	80
10 Heat capacity of $\text{LuCl}_3 \cdot 6\text{H}_2\text{O}$ in the temperature region of the anomaly	82
11 Magnetic heat capacity of $\text{TbCl}_3 \cdot 6\text{H}_2\text{O}$	97
12 Magnetic heat capacity of $\text{HoCl}_3 \cdot 6\text{H}_2\text{O}$	99
13 Difference function relating the present and some previously published $\text{GdCl}_3 \cdot 6\text{H}_2\text{O}$ and $\text{HoCl}_3 \cdot 6\text{H}_2\text{O}$ heat capacities	104
14 Precession photographs of a single crystal of $\text{LuCl}_3 \cdot 6\text{H}_2\text{O}$	107
15 Heat capacity of $\text{GdCl}_3 \cdot 6\text{H}_2\text{O}$ in the temperature region below $10^\circ\text{K}$	111
16 Ground state crystal field splittings from optical spectra	114

## I. INTRODUCTION

Because of the fundamental importance of aqueous solutions to human existence and activity, there has been a continuous and general interest in the study of their properties. The study of, in particular, aqueous electrolytic solutions has been aided by the development of theoretical models, e.g., by Debye and Hückel (1923), to explain their behavior. The existence of these models has given rise to considerable experimental work, devoted to the testing of the theoretically predicted values of the various physical properties. This work has resulted in extending the models to more nearly represent reality. It has also resulted in the need for extensive data in the concentration range between infinite dilution and saturation.

The salts of the rare earths form a particularly valuable series of systems for the study of aqueous electrolyte solutions, in that they constitute a series of multivalent electrolytes, of which the members have similar chemical properties. They are also essentially completely dissociated in dilute aqueous solutions and are available in significant quantity and purity. The ions of the "heavy" rare earths are typically trivalent in aqueous solutions. In crystalline solids, the salts with common anions tend to form isostructural series.

The ready availability of kilogram quantities of rare earth salts, with impurity levels of the order of parts per million, has been made possible by techniques developed and practiced at the Ames Laboratory. The chemical similarity of the rare earths arises from the nature of the differences in their electronic structures. The configurations are such that the electrons of the 4f subshells, within which the differences occur, are



extensively shielded by those of the 5s and 5p subshells. Thus, they are largely excluded from participation in chemical bonding.

In recent years, a coherent program of study carried out at the Ames Laboratory has resulted in the determination of many of the physical properties of aqueous rare earth solutions. These properties have been studied as functions of solute concentration, cation radius, anion valence type and species, and temperature. In particular, the work on the thermodynamic properties of the solutions has demonstrated the need for precise thermodynamic data on the crystalline salts. For example, the calorimetrically determined entropies of the rare earth trichloride hexahydrates must be available before the entropies of the cations in the aqueous chloride solutions can be related to one another in a meaningful way. It is desirable to establish such relationships because they are useful in the development of a better understanding of ion-ion and ion-solvent interactions. Most of the previously available thermodynamic data on these particular salts, for example, that published by Hellwege, *et al.* (1961), and by Pfeffer (1962) are inadequate in two respects. First, the heat capacity measurements were not extended to room temperature. Second, the data above 100°K are generally in error by as much as 2%, because of the presence of occluded moisture in the samples. It was therefore desirable to obtain new and more precise heat capacity data in the range 5°K to 300°K.

A further reason for making heat capacity measurements in this temperature range is related to the spectroscopic properties of the rare earth ions. It is characteristic of these ions, in crystalline solids, that the total crystal field splitting of the ground electronic J level is of the order of several hundred wave numbers. Provided that the heat capacity of a

given crystal exhibits no anomalous behavior in the temperature range of interest, and that the thermal excitations of the vibrations of the lattice can be accounted for, the room temperature entropies provide a measure of that splitting. If other information on the energy level structure of the ions, in the crystal under study, is available, as from spectra, it is possible to compare the results of the optical with those of the thermal measurements.

The samples chosen for this work were the trichloride hexahydrates of Gd, Tb, Ho, and Lu. The Gd and Lu salts were used to set upper and lower limits on the lattice contributions, neither salt having a significant magnetic contribution above 14°K.  $Gd^{+3}$  has, to a first approximation, an  $^8S_{7/2}$  ground state, which is not split by a crystal field. Interaction with higher  $J=7/2$  states may, however, result in a non-degenerate ground state for the ion in the crystal. The ground state of  $Lu^{+3}$  is  $^1S_0$ . The heat capacity of the corresponding salt contains no magnetic contribution.

## II. LITERATURE SURVEY

It is intended that this review be indicative of the relationship between the research to be presented here and that already available in the literature. The alternative, being an exhaustive and critical examination of the literature, would be a project of considerable ambition and would in any case detract from the stated purpose.

In order to suggest the diversity of interests upon which this research has touched, it will be useful to mention some of the reviews and monographs available. These works serve as guides to the more influential of the original literature in their several areas. Moreover they provide insights into the directions taken during the development of their fields.

A standard work on the physical properties of electrolytic solutions is that of Harned and Owen (1943). Another useful book is that by Robinson and Stokes (1955), who emphasize the transport properties of electrolytes. The properties of rare earth ions in aqueous solutions have been discussed by several authors, notably Spedding and Atkinson (1959), Krumholz (1964), and Moeller, et al. (1968). The spectroscopic properties of the rare earth ions have been the subject of a great deal of research, which has been recently reviewed by Dieke (1968). Much of this work has been discussed by Garstein (1960), who has also reviewed work done on the heat capacities of rare earth salts up to about 1960. The subject of low temperature calorimetry has been treated by Westrum et al. (1968). The book by White (1968) is a standard reference on the practical aspects of low temperature work of all types. This brief listing suggests the scope of the material to be discussed during the rest of this review.

Among the most significant early contributors to the development of the theory of ionic solutions were: Arrhenius (1887), who established the existence of ions immediately upon the dissolution of electrolytes, Lewis (1901, 1907) who introduced activities and activity coefficients to measure deviations from ideality, and Milner (1912, 1913) who attempted a first principles calculation of the energy relationships involved in a distribution of positive and negative ions in a given volume. Of particular interest with regard to this last mentioned author, is that he implied, but did not state, that, for 1-1 electrolytes, his energy expression reduced, at very small concentrations, to a form dependent upon the square root of the concentration. This functional dependence upon the solute concentration has been one of the more useful features of the theory of ionic solutions. In 1923 Debye and Hückel (1923a, 1923b) introduced the concept of the "ionic atmosphere" which resulted in simple closed expressions for the behavior of the mean activity coefficient and related thermodynamic properties in the limit of infinite dilution. The validity of their development as a limiting law, its conceptual simplicity and its ready adaptability to comparison with experiment insured its immediate and lasting popularity. Thus, in comparing the work of Milner with that of Debye and Hückel, Noyes (1924) noted the relative unavailability of the former's treatment to those with "---ordinary mathematical training." Further, the appeal of a "mean distance of closest approach" in the Debye-Hückel theory as a concept upon which to rest intuitive arguments about the behavior of electrolytes is evident in the paper of La Mer and Goldman (1929).

The early development of electrolytic solution theory, extensions and critiques of the work of Debye and Hückel, and the theory's later development

up to the mid 1950's have been reviewed by Atkinson (1956). With regard to the transport properties of electrolytes, it is pertinent here to note only that a valid limiting law for electrolytic conductance was developed by Onsager (1927). This work was extended to a more general treatment of the motion of ions by Onsager and Fuoss (1932).

Subsequent to the appearance of the Debye-Hückel theory a great deal of interest developed in the interpretation of experimental results. Harned and Owen (1943) summarized much of this work. They also noted the philosophy that has logically, though not chronologically, guided the development of work in this field. That is, progress in the understanding of ionic solutions requires consideration of the effects of the forces of attraction between ions on all the known properties of the solutions. Experimental verification of the predicted values of the various properties, or conversely, lack of verification, promotes further development of the theory. A prerequisite for the testing of the conclusions of the theory is the existence of a class of strong electrolytes which are essentially completely dissociated at moderate concentrations.

With the development of a ready supply (Spedding and Daane, 1961) of high purity rare earth salts, a good example of such a class of electrolytes became available. The predominating variable across the rare earth series is the ionic radius, which generally decreases with increasing atomic number. This leads, as in the case of the trichloride hexahydrates, to small, regular changes in otherwise isostructural crystals. That, plus the chemical properties of the trivalent ions in solution, suggests the possibility of obtaining a great deal of data on a wide range of physical properties, several of which might be uniquely sensitive to one or another

of the approximations built into the theories of the behavior of electrolytes. In this context, the rare earths thus constitute a series with which it is highly desirable to work. Observations of this sort were made by Spedding, Porter, and Wright (1952a) in the introduction to the first of a series of papers in an extensive program of investigations of the properties of aqueous rare earth solutions. This work will be discussed in topical order. Although such separation is artificial in the sense that there is considerable overlap, it will correlate work that is most obviously mutually related.

The electrical conductivity of ionic solutions is of interest because, in sufficiently dilute systems, the ionic conductance is related to the mobility of ions and to their effective size. Therefore conductance measurements can be used to study e.g., the extent of hydration of ions. The above mentioned paper reported measurements of equivalent conductances of eight rare earth chlorides in the concentration range  $4 \times 10^{-4}$  to 0.1N.  $\Lambda^{\circ}$  as a function of rare earth atomic number was approximately constant from La to Nd and decreased for the rest. The possibility of a change in hydration number was cited. Spedding and Yaffe (1952) measured the equivalent conductances of a series of the bromides with similar results. They reported that the Onsager limiting law was obeyed up to  $10^{-3}$ N. Spedding and Dye (1954) repeated some of the previous chloride measurements to study the effect of hydrolysis. Dye and Spedding (1954) applied graphical integration techniques to Onsager's theory and, in so doing, extended the agreement with experiment to approximately  $10^{-2}$ N. Spedding and Jaffe (1954a, 1954b) studied the equivalent conductances of ten sulfates, eight perchlorates, and three nitrates. They obtained poor agreement with theory with

the sulfates and interpreted this in terms of formation of complexes of the type  $(MSO_4)^+$  in dilute solutions. Heiser (1958) obtained conductances for the nitrates of some intermediate and heavy rare earths. He correlated his work with that of Jaffe and observed behavior, relative to atomic number, similar to that reported for the chlorides. Nelson (1960) measured the conductances of Tb bromide and chloride solutions at concentrations below 0.4N. The values of  $\Lambda$  and  $\Lambda^0$  for the bromides were generally higher than for the chlorides. Saeger (1960) extended the conductance measurements into the moderate and high concentration ranges. He studied the chlorides of several light, intermediate, and heavy rare earths between 0.06N and saturation. Except for La and Nd, the equivalent conductance was a generally decreasing function of atomic number. Further,  $\Delta\Lambda$  was greater in the middle of the series than at either end. Conductance studies carried out prior to the present program included the work of Noyes and Johnson (1909) who attempted with little success to interpret the equivalent conductances of La nitrate and sulfate as functions of concentration. Also, Jenkins and Monk (1950) reported conductance measurements on La sulfate below  $2 \times 10^{-3}N$  and a dissociation constant of  $2.4 \times 10^{-4}$  for the equilibrium  $LaSO_4^+ \rightleftharpoons La^{+3} + SO_4^{-2}$ . There was also the work of Jones and Bickford (1934) who compared the equivalent conductance of La chloride below 1 molar with the predictions of Kohlrausch's law and of Onsager's theory.

Activity coefficients are of interest because they are readily determined theoretically in the limit of infinite dilution, and more fundamentally because they serve to interrelate all of the interesting partial molal properties. They are necessary for a complete thermodynamic description of the system. Transference numbers are related to ionic mobility, but they

are also required for the determination of activity coefficients in dilute solutions, i.e. by the measurement of the potentials of concentration cells with transference. Therefore, these two properties will be discussed together.

Spedding, Porter, and Wright (1952b) reported transference numbers for eight chlorides up to 0.1N. The cation transference numbers were linear in the square root of the normality, but their limiting slopes differ from those predicted by the Onsager theory. They also reported (1952c) activity coefficients in the same concentration range, and obtained good agreement with the predictions of the Debye-Hückel theory. The transference number results were in good agreement with the earlier work of Longworth and MacInnes (1938) on La chloride. Further transference number and activity coefficient results were published by Spedding and Yaffe (1952) on the bromides, Spedding and Dye (1954) on the chlorides, and Spedding and Jaffe (1954b) on the perchlorates and nitrates. With respect to the activity coefficients, a remarkable agreement between theory and experiment resulted, in part, from treating the "mean distance of closest approach" as an experimentally determined parameter which was then used in the calculation of  $\gamma_{\pm}$ . Also, Spedding and Dye (1954) reported improved agreement between the transference number results and the predictions of theory when the latter were obtained on the basis of their graphical integration approach (Dye and Spedding, 1954). Heiser (1958) reported transference numbers and activity coefficients for the nitrates of Sm, Ho, Er, and Yb up to 0.2N. He noted that  $\gamma_{\pm}$  as a function of concentration behaved anomalously for the Ho salt and suggested that the cause might be complex formation. Nelson (1960) reported these data for Tb bromide and chloride below 0.2N, and noted the



variations in the limiting transference numbers with atomic number for the rare earths studied to that time, i.e. most of the chlorides and bromides. Saeger (1960) reported activity coefficients from 0.1N to saturation for a number of rare earth chlorides representative of the series. In general, he found good agreement between his and earlier work by Robinson (1937, 1939), by Mason (1938, 1941), and by Heiser (1958). The comparison with Mason's results suggested discrepancies in the composition of that author's solutions, i.e. oxychloride formation. Saeger noted that the functional dependence of his activity coefficients on concentration indicates increasingly strong ion-solvent interactions at high concentrations. Other noteworthy work on the activity coefficients of rare earth chlorides includes that done earlier by Shedlovsky and MacInnes (1939) and by Shedlovsky (1950) on dilute solutions of La chloride. Of historical interest is the work of Hall and Harkins (1916) who used the first commercially produced White Double Potentiometer in freezing point studies of La nitrate solutions.

Measurements of partial molal volumes yield information about the changes which occur in solution volume upon the addition of solute. They are of interest therefore in the study of ion-solvent interactions, e.g., the packing of solvent molecules about the solute ions with attendant reduction in effective solvent volume. For this reason the program under consideration has included considerable study of partial molal volumes and related properties.

Spedding, Pikal, and Ayers (1966) have recently published the results of investigations of apparent and partial molal volumes of the chlorides of La, Pr, Nd, Sm, Gd, Tb, Dy, Ho, Er, and Yb and the nitrates of La, Er, Nd,

and Yb in the concentration range  $2 \times 10^{-3} < m < 0.2$ . It is indicated that at infinite dilution the partial molal volumes of these systems are additive properties of the individual ions, as expected for completely dissociated solutes. The limiting values of the solute partial molal volumes form two distinct groups when plotted as a function of atomic number. There is a general decrease from La to Nd followed by a strong increase to Gd, with Sm approximately intermediate. After Gd and Tb, there is again a gradual decrease. The gradual decreases are interpreted as being due to the increasingly close packing of  $H_2O$  molecules in the first hydration sphere about the increasingly small, highly charged rare earth ions. Following this line of thought, the sudden increase in  $\bar{V}_2^0$  is the effect of the loss of a water molecule from the first hydration sphere. The fact that the change is not completely discontinuous is considered to be due to a shifting equilibrium between two possible coordination numbers. The higher coordination number is said to be favored for the larger ions, with the lower being favored from Tb onward. Atkinson (1956) measured the compressibilities of the chlorides and nitrates of La, Nd, Er, and Yb in the concentration range  $m < 0.5$ . He noted that the agreement between experimental partial molal volumes and those calculated from theory, previously poor, was improved by approximately 15% when the solution compressibility was considered in the theory. His apparent molal compressibility values reflected a decreased compressibility of the solution relative to the pure solvent due to the close packing of the  $H_2O$  molecules about the rare earth ions. He also suggested the possible existence of an equilibrium between two first hydration sphere coordination numbers within the rare earth series. However Ayers appears to be the first to explicitly state this postulate. Gildseth (1964) measured

density as a function of concentration and temperature, in the ranges  $0 < m < 3.4$  and  $20^{\circ}\text{C} < T < 80^{\circ}\text{C}$ , for La and Nd chloride solutions. He reported partial molal volumes and expansibilities at various concentrations and temperatures. Correlation of these results with those of Saeger (1960) indicated that the behavior of  $\bar{V}_1$  is consistent with strong orientation of the  $\text{H}_2\text{O}$  dipoles toward the rare earth ions. It is expected that  $\text{H}_2\text{O}$  molecules beyond the first hydration layer are also bound to the ion and ordered to a considerable extent. He further noted that while the expansibility and compressibility results were consistent with this point of view, those from conductance and transference number measurements were ambiguous.

A systematic investigation of the physical properties of a class of electrolytes necessarily includes the obtaining of a large amount of thermal data. Spedding and Miller (1952a) measured the heat capacities and enthalpies of solution and dilution of the (anhydrous) chlorides of Ce and Nd. The concentration range of the dilution measurements extended up to 0.4 molal. The agreement with the limiting law predictions was to within experimental error below 0.002 molal. They noted that the heat of solution to infinite dilution is a measure of the difference between the lattice energy of the crystal and the hydration energy of the ions. Comparison of these data for two members of an isostructural series of, say chlorides, allows a correlation to be drawn between hydration energy and ionic radius. They also reported (1952b) heats of solution for the hydrated chlorides of Ce and Nd. They used these data, standard electrode potentials for Ce and Nd, and the methods of Latimer (1951) to estimate the aqueous entropies of the ions. Spedding and Flynn (1954a, 1954b) measured the heats of solution of some of the rare earth metals and of the anhydrous chlorides of La, Pr,

Ce, Sm, Gd, Er, Y, and Yb. They made similar measurements on the hydrated chlorides of La, Pr, Sm, Gd, Y, Er, and Yb. The heats of solution of the hydrates formed three groups as a function of atomic number. The results for the heptahydrates and for the hexahydrates to Gd formed two groups, while those for the Er and Yb salts formed the third. The authors suggested that the anomalous Er and Yb results were due to a structural change for these salts relative to the lighter members of the series. A more likely explanation stems from Pepple's (1967) observation that Flynn's calorimeter, designed for work on the metals, was not sufficiently sensitive to the relatively smaller solution enthalpies of the hydrates. Spedding, Naumann, and Eberts (1959) reported the heat of solution of the hydrated Nd chloride and the heats of dilution below 0.2 molal for La, Nd, Er, and Yb chloride and for La and Yb nitrate solutions. They found that the measured apparent molal heat contents of the lighter chlorides and nitrates agreed with the limiting law predictions but that those of the heavier rare earths did not. They suggested that this was due to hydrolysis in the extremely dilute solutions for which  $\text{pH} > 5$ . Bisbee (1960) measured the heats of solution of Tm, Lu and anhydrous  $\text{LuCl}_3$  in HCl, and of anhydrous Tm and Lu chlorides to infinite dilution in water. The non-linear behavior of the heats of solution of the chlorides, of this and previous work, as functions of rare earth atomic number was due to a variation in the crystal structure of the salts across the series. Csejka (1961) and DeKock (1965) measured the heats of dilution of a large number of chlorides representative of the series, and published their results jointly (Spedding, Csejka, and DeKock, 1966). The limiting slopes of the apparent molal heat contents from their data generally agreed well with the predicted values. The  $\phi_L$  values from this and previous

work, plotted as functions of atomic number, formed separate groups for the light and heavy rare earths with Sm and Gd results intermediate. This effect was qualitatively discussed in terms of the functional dependence of  $\Phi_L$  on the mean distance of closest approach in the Debye-Hückel limit. A discrepancy between these results and  $\Phi_L$  obtained from heat of solution work on the anhydrous chlorides, suggested a relatively long-lived metal-chloride complex, to the existence of which the heat of solution calorimetry was insensitive. This postulate was supported by the much better agreement found between the  $\Phi_L$  values and those obtained from the heat of solution work on the trichloride hexahydrates of Nd and Dy. Spedding and Jones (1966) published the results of heat capacity measurements of the chlorides of La, Nd, Eu, Er, and Yb in the concentration range 0.1 molal to saturation. These values were consistent with a change in the first hydration sphere coordination number across the series. They noted that factors relatively unimportant in dilute solutions, such as complex formation, became increasingly important to the measured properties at high concentrations. X-ray diffraction measurements, conducted by Brady (1960) on Er chloride and iodide solutions, suggested the existence of considerable metal-halide ion pairing at concentrations above ~ 1 molar. Walters (1968) has recently measured the heat capacities, at concentrations above 0.1 molal, for the chlorides of Pr, Sm, Eu, Gd, Tb, Ho, Tm, and Lu, the nitrates of La, Nd, Gd, Er, and Lu, and the perchlorates of La, Nd, Gd, and Lu. The apparent molal heat capacities formed two series for the chlorides and perchlorates. The author commented on the need for more data on the nitrates. For the solutions of the heavy rare earths, the solvent partial molal heat capacities showed a sharp increase at high concentrations, i.e.  $m^{1/2} \sim 1.9$ .

This was explained qualitatively as being the result of an anion entering the first hydration sphere of the metal, dislodging a  $H_2O$  molecule and simultaneously reducing the net surface charge density of the hydrated complex. Each of these processes would contribute to an increase in  $\bar{C}_{p1}$  by increasing the freedom of movement of the hydrated  $H_2O$  molecules. The chloride solutions of Gd, Tb, and Ho from Walter's work were the source of the crystals grown for the research to be reported by the present author. Pepple (1967) has measured the heats of dilution of the chlorides of Nd, Sm, Eu, Gd, Dy, Er, Tm, and Lu from infinite dilution to saturation. He has also measured the heats of solution of the hydrated chlorides of La, Pr, Nd, Sm, Gd, Dy, Er, Tm, Yb, and Lu and tabulated the values of the heats of solution and partial molal excess entropies of these and of the corresponding Tb and Ho salts. These last values were based on the work of DeKock (1965). The heats of solution as functions of rare earth atomic number formed two groups rather than three as observed by Spedding and Flynn (1954a, 1954b). In this more recent work, the discontinuity occurs between Pr and Sm. Following Eu, the values fall on a smoothly increasing curve to Lu.

Some other measurements of the solution thermal properties of the rare earths will be noted. These include the work of Matignon (1906a, 1906b) on the heats of solution of, e.g., the trichloro hydrates of Pr and Nd, and that of Bommer and Heumann (1941) on the heats of solution of a number of the metals in HCl. Nathan, Wallace, and Robinson (1943) reported some of the first work on the heats of dilution of 3-1 electrolytes in their study of La chloride solutions below 0.025 molal. They also studied the sulfate system. Lohr and Cunningham (1951) reported the standard enthalpies of

formation of the aqueous La and Pr ions. Their work involved the use of rare earths as "stand-ins" during the development of procedures for the preparation and characterization of Am. Lange and Miederer (1956) measured heats of dilution of La nitrate solutions, and Sieverts and Gotta (1928) the heat of solution of La and Pr. Jekel, Criss, and Cobble (1964) have recently studied the temperature dependence of the partial molal heat capacity of dilute solutions of Gd chloride in the range  $0^{\circ}\text{C} < T < 100^{\circ}\text{C}$ . Their results are expected to be only approximate, since they involve an estimation of the heat capacity of the anhydrous crystal based on an extrapolation of the published heat capacity of the trichloro hexahydrate. These latter values (Hellwege et al., 1961) are incorrect in the temperature range  $100^{\circ}\text{K} < T < 300^{\circ}\text{K}$  by as much as 2%, as will be shown in a later section.

The trends across the rare earth series, observed in a number of the properties already discussed, have also been found in the standard heats of formation of some chelates. Mackey, Powell, and Spedding (1962) reported standard enthalpies, free energies and entropies of formation for the rare earth-EDTA complexes based on calorimetrically determined heats of reaction. The enthalpy changes form two groups, with the transition occurring at approximately Eu. Their results also showed the considerable contribution of the entropy term to the stability of the rare earth complexes. Thus for the complex Gd-EDTA,  $(-)\Delta F_f^{\circ}$  is approximately 23 kcal/mole and  $(-)\Delta H_f^{\circ}$  and  $\Delta S_f^{\circ}$  are of the order of 1.7 kcal/mole and 71 cal/mole respectively. Similar measurements had been reported previously by Betts and Dahlinger (1959) who determined the enthalpy changes from the temperature dependence of the stability constants. They suggested a change in coordination number of the metal ion with respect to the chelate as a means of explaining the trends in

their entropy values. Mackey, Powell and Spedding (1962) have argued against this interpretation since, e.g., the trends observed in the enthalpies of formation are essentially independent of the chelating agent. Edelin De La Praudiere and Staveley (1964) have observed irregular trends across the rare earth series in the heats of formation of the nitrilotriacetate complexes. The factors which are important to complex formation and to the stability of complexes have been discussed by Grenthe (1964). He suggested that the large entropies of formation result from a breakdown in the ordered arrangement of the  $H_2O$  molecules around the hydrated metal ion, due to the presence of the ligand.

The work on solution properties discussed here, especially that of Spedding and Miller (1952b), and the general interest in rare earth complexes have illustrated the desirability of having calorimetric data on, e.g., the crystalline rare earth trichloride hexahydrates. The only high temperature data presently available are contained in a series of papers published by Hellwege and his co-workers (Hellwege et al., 1959, 1961, 1962; Pfeffer, 1961a, 1961b, 1962). The temperature ranges covered by these heat capacities generally exclude room temperature. For the La and Pr crystals (Hellwege, et al., 1959), the measurements extend up to  $280^{\circ}K$ , but with respect to the others the highest temperature reported was  $260^{\circ}K$  for the Gd salt (Hellwege et al., 1961). In general, data were given in the range  $1.5^{\circ}K \leq T \leq 220^{\circ}K$ . Implicit in this is the presence of an error, in all of their data, caused by occluded solution in their crystals. In particular, Hellwege, et al. (1961) noted that the  $GdCl_3 \cdot 6 H_2O$  sample contained excess moisture amounting to  $\sim 0.2\%$  of the sample weight.

The effect of occluded moisture on the heat capacities of crystalline



hydrates has been recently studied by Gerstein (1960) in the case of the ethylsulfates of Tm and Lu. These results indicated that the errors became significant at temperatures at least above 220<sup>o</sup>K. Above this temperature the excess water manifests itself in a broad bump in the plot of  $C_p$  as a function of T, extending to approximately the ice-point. The maximum in this bump lies as much as several percent, (in  $C_p$ ), above the "true" curve. Therefore, values obtained by extrapolation of data in this temperature range will be consistently too large. The data cannot be corrected for this error since the low temperature heat capacity of the saturated solutions are generally unknown. Because of the wide interest in the thermodynamic properties of these rare earth salts, it was considered desirable to redetermine the heat capacities of a series of trichloro hexahydrates. It is expected that knowledge of  $S_{298}^o$ , combined with presently available solution data (Pepple, 1967), will lead directly to the determination of rare earth ionic entropies.

It is characteristic of the rare earth ions in crystalline solids, that for those electronic ground states for which the degeneracy is removed by interaction with a crystalline electric field, the total splitting of the components produced by such interaction is of the order of  $kT$  at room temperature. The implication is that thermal data i.e., magnetic entropies as determined from heat capacity measurements, are a measure of the crystal field splittings of the rare earth ions. Spectroscopically determined ground state components, for the rare earth ions in two of the salts of particular interest in this present study, are available in the literature. Dieke (1968) have tabulated values for the thirteen-levels in the  $^7F_6$  state of  $Tb^{+3}$  in  $TbCl_3 \cdot 6 H_2O$ , determined from the fluorescence spectrum.

Kahle (1956) has published values for the lowest four levels in the  $^5I_8$  state of  $\text{Ho}^{+3}$  in  $\text{HoCl}_3 \cdot 6\text{H}_2\text{O}$  observed in absorption. He noted that at sample temperatures such that the next higher components would be significantly populated, the absorption bands became too broad for resolution of the levels. An opportunity therefore exists to study the contribution to the entropy from the thermal population of these levels, and to compare that obtained from calorimetry to that calculated from the spectroscopically determined levels.

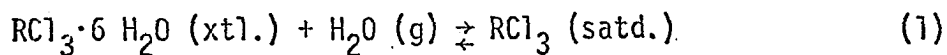
### III. EXPERIMENTAL DETAILS

#### A. Samples

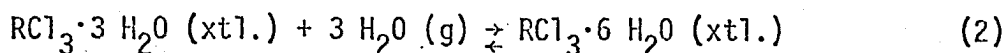
As has been mentioned, the crystalline trichloride hexahydrates of Gd, Tb, and Ho were prepared from the solutions used by Walters in his solution heat capacity measurements. The crystals of Lu trichloride hexahydrate were grown from a solution prepared by dissolving the metal oxide in an excess of reagent grade HCl. The oxide was obtained from the Ames Laboratory's rare earth separations group. During the preparation of the hydrates, steps were taken to minimize the effects of hydrolysis, oxychloride formation, and the occlusion of saturated solution by the crystals. Prior to the heat capacity measurements, samples of each of the salts were analyzed chemically, and emission and mass spectroscopically.

Gerstein has shown that the heat capacity of a crystalline hydrate is sensitive to the presence of excess water in the sample. It was therefore necessary to give considerable attention to the problem of occlusion and absorption of moisture. This problem will be briefly discussed in order to make the sample preparation procedure more meaningful.

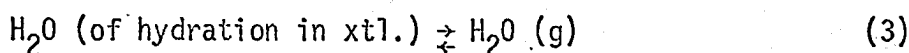
The situation that exists when the hydrate is formed, reversibly, from the saturated solution is:



This is a two component, three phase system, for which the equilibrium vapor pressure is fixed by the temperature. If the system loses water and goes, reversibly, to a lower hydrate, say the trihydrate, the situation is represented by:



The equilibrium vapor pressure for this system is also fixed at a given temperature. Between the extremes represented by equations 1 and 2, the crystalline hexahydrate co-exists in equilibrium with its vapor. This equilibrium is represented by:

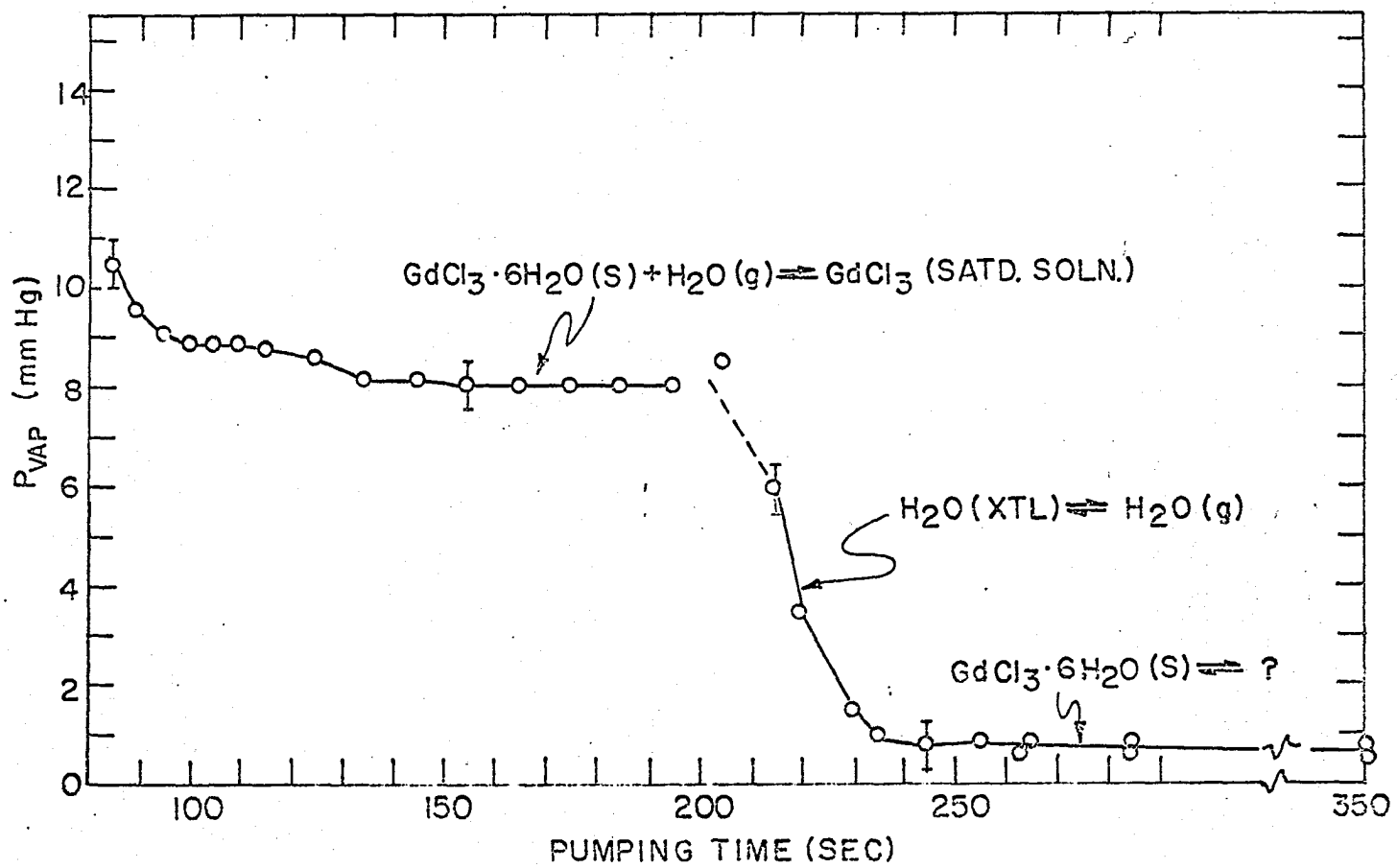


At a given temperature, there will be a range of vapor pressures within which this situation may obtain.

One may observe the vapor pressure as a function of the relative solute concentration, as in Figure 1 for the case of  $\text{R} \equiv \text{Gd}$ . These data were obtained by monitoring the pressure over the solution while pumping water away to a cold-trap. The equilibria represented by equations 1 and 3 are indicated in the figure. If water in the crystals is allowed to come to equilibrium with water vapor at a pressure below the vapor pressure of the saturated solution and above that of the decomposition products, the crystals will contain no excess moisture. Because of the total absence of the solution phase, the heat capacity will be that of the stoichiometric hexahydrate. The situation which exists in the lowest portion of the curve in Figure 1 is probably more complex than that represented by equation 2.

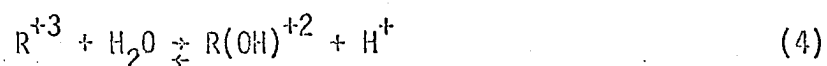
Haeseler and Matthes have studied the thermal decomposition of a number of the rare earth trichloride hexahydrates, in particular, those of Gd, Tb, and Ho. They found that "in air", these salts were stable with respect to the next lower hydrates at temperatures at least as high as 50°C. In atmospheres consisting of air-HCl mixtures, these temperatures were of the

Figure 1. Vapor pressure as a function of solute concentration for the  $\text{PCl}_3 - \text{H}_2\text{O}$  system



order of 70<sup>0</sup>-90<sup>0</sup>C. The stability also tended to increase with rare earth atomic number. The ultimate decomposition products observed were the oxychlorides, which became stable at temperatures of the order of 200<sup>0</sup>-300<sup>0</sup>C. Intermediate were a series of tri-, di-, and mono-hydrates, stable over various temperature ranges.

Saeger (1960) has determined the equivalence pH at 25<sup>0</sup>C for the hydrolysis reaction:



He has found it to be of the order of unity for the saturated solutions of the heavy rare earth chlorides.

In order to prepare the crystalline hexahydrates, the chloride solutions were slowly evaporated over a period of weeks. During this time, the temperatures and the pH values of the solutions were maintained at 45<sup>0</sup>C and within the range 0.5-1.5 respectively. The crystals, when formed, were allowed to remain in contact, at room temperature, with the saturated solutions for periods of the order of a week. The crystals were removed by filtration, crushed, and placed in desiccators over CaCl<sub>2</sub> solutions to "equilibrate". The concentrations of the CaCl<sub>2</sub> solutions were adjusted, using the data of Kolthoff and Sandell (1952) so that their equilibrium vapor pressures were within the range such that only water vapor and hexahydrate could co-exist in equilibrium at room temperature. The crystals were periodically crushed to produce increasingly fine powders. This procedure guaranteed more rapid equilibration in the desiccators and improved the thermal contact of the samples during the heat capacity measurements.

Prior to the heat capacity measurements, portions of the samples were

analyzed chemically as a check on the waters-of-hydration concentration. The analyses were performed under the supervision of Robert Bachman of Analytical Chemistry Group I. The values of "n" in  $RCl_3 \cdot n H_2O$  were found to be:  $6.1 \pm 0.1$  for  $R \equiv Gd$ ,  $5.9 \pm 0.1$  for  $R \equiv Tb$ ,  $5.9 \pm 0.1$  for  $R \equiv Ho$ , and  $5.9 \pm 0.1$  for  $R \equiv Lu$ . Other portions of the samples were converted to the oxides and submitted to Analytical Services Group II for emission spectrographic and to Analytical Group III for mass spectrographic analyses. The results of these determinations are presented in Tables 1 and 2.

Table 1. Results of emission spectroscopic analyses (impurities in PPM by weight)

Element	$Gd_2O_3$	$Tb_4O_7$	$Ho_2O_3$	$Lu_2O_3$
Nd	<100			
Sm	<100	<200		
Eu	<100	<20		
Gd		<200		
Tb	<500			
Dy	<50	<100	<150	
Ho	<200	<100		
Er			<500	160
Tm			<200	<10
Yb			<<50	~17
Sc				<5
Y	<500	<50	<100	<10
Fe	<10	60	<50	<30
Al	60	50	10	10
Ca	<10	40	<10	200
Si	<10	<20	40	145
Ta				<200
Mg				<10
Cu				<10
Ni				<10
Cr				<10



Table 2. Results of mass spectroscopic analyses (impurities in PPM, atomic)

Element	Gd <sub>2</sub> O <sub>3</sub>	Tb <sub>4</sub> O <sub>7</sub>	Ho <sub>2</sub> O <sub>3</sub>	Lu <sub>2</sub> O <sub>3</sub>
Be	0.5	2.0	0.7	
B	0.8	2.0	1.0	
F	7.5	9.0	5.0	
Na	6.5	2.0	5.0	
Al	3.5	4.0	7.0	
Si	45.0	30.0	40.0	
P	0.45	1.0	0.8	
S	≤2.0	≤4.0	≤0.7	
Cl	45.0	300.0	150.0	40.0
K	1.5	4.0	0.6	0.4
Ca	30.0	30.0	6.0	200.0
Sc	≤1.0	≤1.0	N.D.	1.0
Ti	≤1.0	≤1.0	<1.0	
V	0.25	≤1.0	0.5	≤0.3
Cr	0.65	0.5	0.2	0.5
Mn	0.35	0.5	Interference	0.4
Fe	1.6	0.5	0.1	0.8
Co	0.008	0.9	0.01	0.1
Ni	0.27	0.3	0.1	
Cu	0.75	1.0	0.4	2.0
Zn	10.05	0.5	0.2	2.0
Ga	≤0.03	≤0.1	≤0.02	
Ge	N.D.	N.D.	N.D.	
As	≤0.06	N.D.	N.D.	
Se	N.D.	N.D.	≤0.2	
Br	N.D.	N.D.	≤0.2	
Rb	N.D.	N.D.	N.D.	
Sr	N.D.	N.D.	N.D.	
Y	9.0	400.0	5.0	0.5
Zr	0.7	N.D.	≤1.0	
Nb	<3.0	<5.0	<1.0	
Mo	N.D.	N.D.	N.D.	
Ru	0.3	N.D.	N.D.	
Rh	N.D.	N.D.	N.D.	
Pd	N.D.	N.D.	N.D.	
Ag	0.02	N.D.	0.2	
Cd	N.D.	N.D.	N.D.	
In	N.D.	N.D.	N.D.	
Sn	N.D.	N.D.	0.7	
Sb	N.D.	N.D.	N.D.	
Te	N.D.	N.D.	N.D.	
I	N.D.	N.D.	N.D.	
Cs	N.D.	N.D.	0.01	
Ba	0.25	0.6	0.1	
La	0.35	4.0	1.0	0.2

Table 2. (Continued)

Element	Gd <sub>2</sub> O <sub>3</sub>	Tb <sub>4</sub> O <sub>7</sub>	Ho <sub>2</sub> O <sub>3</sub>	Lu <sub>2</sub> O <sub>3</sub>
Ce	0.6	0.3	1.0	≤0.6
Pr	0.6	0.5	2.0	≤2.0
Nd	1.2	6.0	2.0	0.7
Sm	2.0	2.0	1.0	≤0.4
Eu	0.5	0.4	0.4	≤0.08
Gd	10 <sup>6</sup>	≤20.0	10.0	≤0.2
Tb	N.D.	10 <sup>6</sup>	2.0	≤0.05
Dy	3.0	2.0	2.0	0.4
Ho	<10.0	5.0	10 <sup>6</sup>	0.2
Er	2.0	N.D.	N.D.	0.8
Tm	3.0	0.2	N.D.	0.2
Yb	<20.0	20.0	1.0	1.0
Lu	2.0	<5.0	0.3	10 <sup>6</sup>
Hf	≤0.5	N.D.	2.0	
Ta	≤1.0	0.4	6.0	
W	≤1.0	N.D.	N.D.	
Re	N.D.	N.D.	N.D.	
Os	N.D.	N.D.	N.D.	
Ir	N.D.	N.D.	N.D.	
Pt	N.D.	N.D.	N.D.	
Au	N.D.	N.D.	N.D.	
Hg	N.D.	N.D.	N.D.	
Tl	N.D.	N.D.	N.D.	
Pb	1.0	2.0	0.6	3.0
Bi	N.D.	N.D.	N.D.	
Th	0.5	N.D.	N.D.	150.0
U	N.D.	N.D.	N.D.	

### B. Apparatus

The equipment directly associated with the measurement of heat capacities from liquid helium to room temperatures can be conveniently discussed in terms of its several constituent parts. Each of these is associated with a specific function. It is felt, therefore, that descriptions of each of the components and of their relationships to one another will also say quite a bit about the measurement as a whole. The calorimetric apparatus itself

can be broadly broken down into: the calorimeter<sup>1</sup>, the adiabatic shield control system, the thermometer and the sample heater, with their associated wiring and power sources, and the measurement station. This last part contains the potentiometer, with which the sample temperatures and sample heating data are measured. It also contains the timing apparatus which controls the heat added to the sample, and the various standard resistors, switches, voltage dividers, and circuitry which are necessary for the measurement. Skochdopole (1954) has described many of the circuits associated with the measuring station. Therefore, only the first three parts and the potentiometer will be considered. Of these four, three were constructed or installed specifically for use in making the measurements reported here.

### 1. Calorimeter

In general, three factors have contributed to a standardization of the design of low temperature calorimeters. These are, first, the long and active history of calorimetry, beginning approximately with the work of Gaede (1902) and Nernst (1910). Secondly, physical requirements, e.g. thermal isolation, limit the number of ways in which a basic design can be varied. Thirdly, the need for measurements of the highest practicable precision from a given laboratory and for the highest attainable degree of reproducibility among laboratories has resulted in the use of similar components and procedures by the various workers in the field.

---

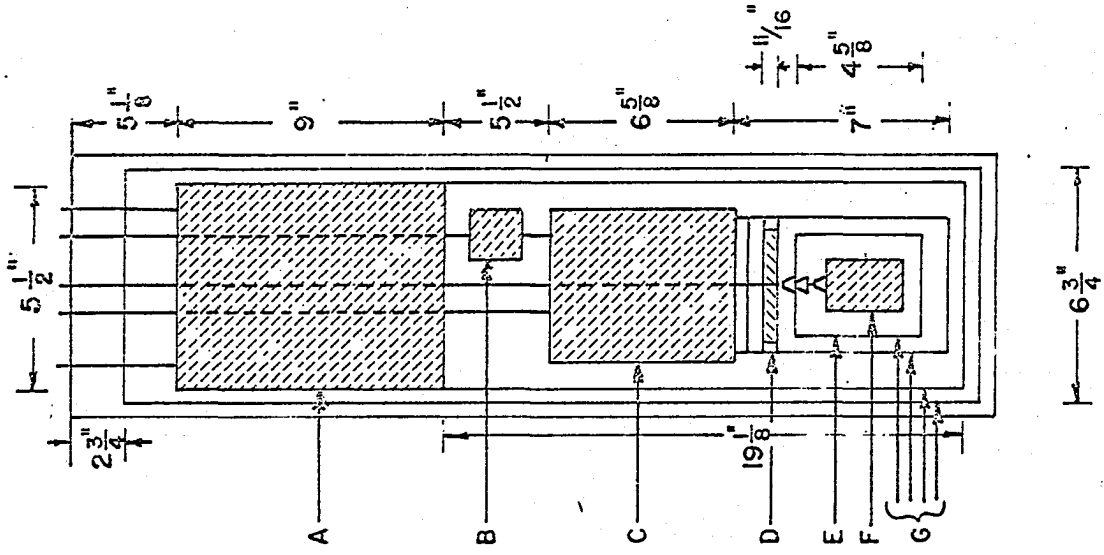
<sup>1</sup>The term "calorimeter" will be used to describe the mechanical part of the apparatus taken as a whole. The term "calorimeter can" or simply "can" will mean the removable component directly containing the sample.

The calorimeter designed and built for this problem is of a widely used type described by Westrum et al. (1968), and pictured in Figure 2 of their article. The resemblance to Figure 2 of the present work illustrates the degree of standardization which exists. Because of the ready availability of descriptive material in the literature, (see also the monograph by White (1968)), this discussion will be limited to the details of interest with respect to this particular instrument:

Figure 2 is a schematic drawing of the adiabatic calorimeter used in this research. For clarity, the smaller components have not been shown. The device consists essentially of a vacuum space, within which are contained: a liquid nitrogen reservoir (A), a liquid helium reservoir (C), and economizer (B), a "floating ring" (D), (henceforth called "RING"), an adiabatic shield (E), a calorimeter can (F), and numerous radiation shields (G). Each of these components contributes specifically to the thermal isolation of the can containing the sample under study, and/or to the control of its temperature. In particular, they are all either gold- or chromium-plated to reduce radiative heat transfer. The liquid inlet and vent tubes are indicated as lines, as is the cable supporting the calorimeter can. The liquid transfer lines, electrical lead inlet, and winch are all located above the top horizontal line in the figure. They are all similar to the corresponding parts of Westrum's apparatus, except for the electrical lead inlet.

A bundle of 41 copper leads (B&S Gauge #34) enters the vacuum space through a seal consisting of two circular plates, between which are pressed two rubber "O-rings" in machined grooves. Approximately 2 meters of slack leads are helically wound in the vacuum space above the nitrogen

Figure 2. Some of the principal features of the calorimeter



reservoir (A). The wires are thermally grounded to the top and bottom of (A), having been separated and glued with G.E. 7031 adhesive. Electrical insulation is provided by S&S weighing paper, which is glued between the wires and the component. Radiation shielding is provided by aluminum foil, which covers the portion of the wires in contact with the reservoir. Another 2 meters of slack leads are interposed between (A) and (B). The function of (B) is to pre-cool the leads before they come into contact with the helium reservoir (C). The leads are thermally grounded to (B) and (C) in the same manner as to (A).

Except for that of the vacuum jacket and one shield, the entire weight of the calorimeter is suspended from the inlet and vent tubes of (A). The strength requirements placed on these lines results in considerable heat transfer to the nitrogen tank and makes it necessary to replenish the liquid daily. The helium reservoir and all components beneath it, except the can, are suspended by a network of 15-pound-test nylon lines from (A). Stainless steel rods were originally used for this purpose, but their presence resulted in a heat leak of approximately  $0.1 \text{ kilocalories hour}^{-1}$  from (A) to (C). Ashworth and Steeple (1968) has recently studied the various contributions to heat transfer in calorimeters of this type. The incorporation of some of his suggestions into this apparatus, including the lining of the inside of the vacuum jacket with aluminum foil has decreased the heat leak such that one liter of liquid helium lasts approximately 23 hours. This performance is, in view of the laboratory's present capability to recover the helium, satisfactory; but the basic design of the calorimeter can still be much improved in this respect. For example, thermal contact between the shields (G) and the reservoirs to which they are grounded can be improved as suggested by Ashworth.

The electrical leads proceed from the bottom of (C) to (D), around which they wrap approximately  $2\frac{1}{2}$  times and to which they are thermally tied. Approximately 12 inches of slack are interposed between (C) and (D). The purpose of the RING (D), is to pre-warm the leads either to the temperature of the adiabatic shield (E) or to some other temperature at the option of the experimenter. After leaving the RING, the leads go to the middle of the adiabatic shield (MASH)<sup>2</sup> around which they are non-inductively wound and thermally tied. Figure 3 shows an exploded view of this portion of the calorimeter in detail. At the bottom of the MASH the bundle of leads is separated into two parts. Those wires used for thermocouple leads pass through a small hole in the MASH, while the rest are attached with low-thermal-e.m.f. solder, (White, 1958), to copper binding posts. These binding posts, passing through the MASH, effectively separate the leads from one another and provide points of attachment inside the shield for the heater and thermometer leads.

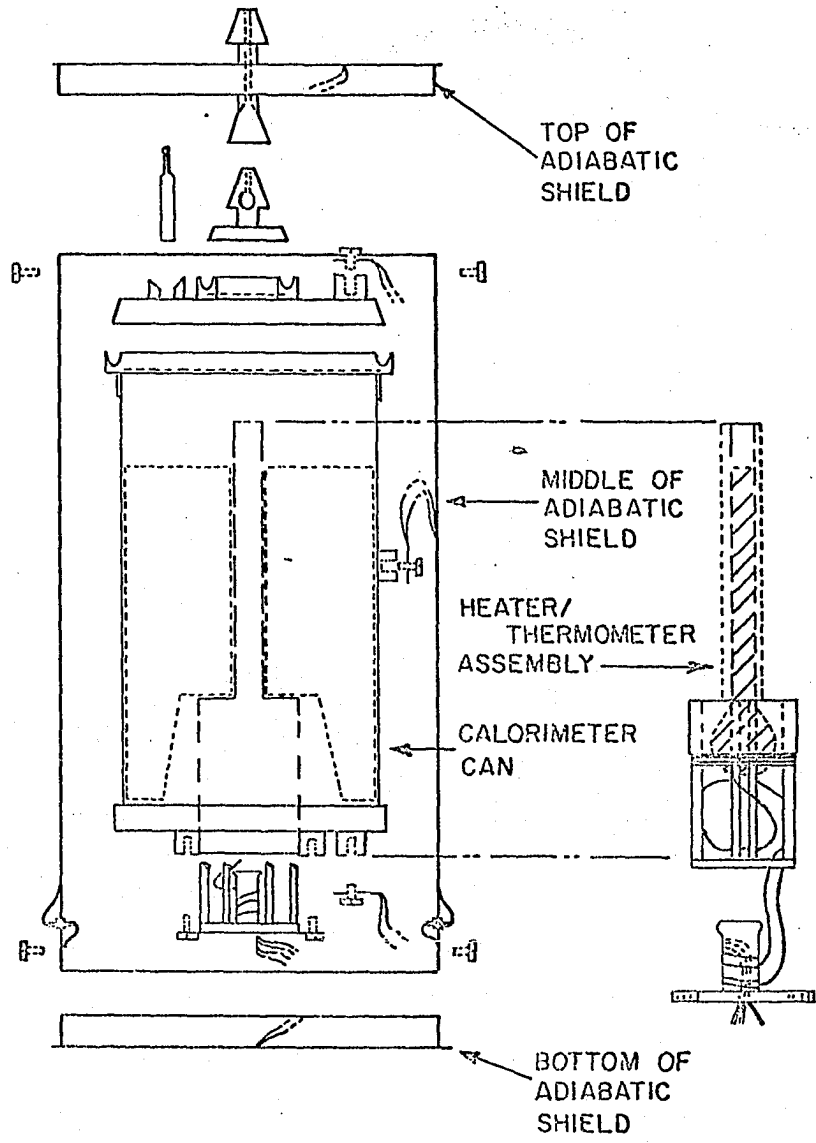
From the binding posts, two leads of #38 copper and one of #36 manganin go to the sample heater, wound in helical grooves on the heater/thermometer shell. The latter is shown on the right in Figure 3. (See also Figure 7 of Westrum's article (1968). Four leads of #38 copper provide electrical contact between the binding posts and the platinum resistance thermometer. Several inches of slack in the lead bundle thermally separate the heater/thermometer shell from the shield. Inside the shell, the leads are wound twice around and glued to a tube on the shell cover. Approximately two

---

<sup>2</sup>The words MASH, TASH, and BASH will, for convenience, be used to specify the three parts of the adiabatic shield. While not universally accepted, they are sufficiently widely recognized to justify their use.



Figure 3. Details of the calorimeter can, adiabatic shield, and heater/thermometer assembly



additional inches of slack wire separate the cover from the thermometer. The heater is further isolated from the outside in that its leads are non-inductively wrapped five times around the 0.05 inch brass support posts of the shell. The heater, #46 Advance, with a resistance of about 300 ohms is kept in place with formex enamel which has been baked onto the assembly. Wherever in the heater/thermometer shell assembly the leads are thermally tied or are soldered to other wires, they are similarly enameled and baked.

The calorimeter can itself is made of 0.025 inch thick copper and consists of a heater/thermometer well, can body, and inner and outer covers. A removable four-bladed thermal contact fin made of the same material is inside the can. The inner and outer covers are attached with bismuth-cadmium eutectic solder (White, 1968, Hansen, 1958). The rather wide grooves are necessary because of the rapid deterioration of the surface of the solder at the melting temperature (about  $140^{\circ}\text{C}$ ). Thermal contact between the can, the TASH, and ultimately the helium reservoir, is obtained by raising the former with the winch via a suspension line made of braided steel cable from a strip-chart recorder, a single loop of 15-pound-test nylon line, and a coiled steel spring between the two. Following the loading of a sample into the can and sealing of the cover, the air can be removed and helium introduced via the silver tube shown to the left of the thermal contact cone. Subsequently the silver tube can be fused shut, as it is shown. It was found that the best technique for performing this last operation is to apply to the end of the silver tube, temporarily pinched shut, the maximum flame attainable from a hand-held oxygen-propane torch for the minimum time necessary. This is routinely of the order of one second. With the exercise of some care this method is consistently successful.

Three multiple junction thermocouples, consisting of manganin/Au-Fe/ chromel-P/Au-Fe sections are attached between the MASH, TASH, and BASH and the corresponding parts of the can. Manganin was used in preference to copper because their thermal conductivities compare approximately as 1:400, at 10<sup>0</sup>K. These thermopiles serve to monitor the temperature differences between the can and shield and are the sensors of the adiabatic shield control system, (either automatic or manual). A similar thermopile monitors the MASH-RING temperature difference. Other thermocouples of the type Au-(2.1 At.%)Co/Cu enable one to monitor the temperature of the shield with respect to that of the helium reservoir. This last is especially useful during liquid helium transfers.

Heat is introduced from the shield control system to the RING, MASH, TASH, and BASH via heaters of 1200, 1000, 3500, and 3900 ohms resistance respectively. The ratios of these resistances were determined by the requirement that all shield components heat at the same rate for the same voltage across each resistor. These resistors are non-inductively wound on their respective components, under the main body of leads in the case of the MASH. In order to insure uniform heating of the components, the heaters are overwound near the edges. Another heater of approximately 750 ohms is wound on the bottom of the helium reservoir and is used primarily to melt solid nitrogen, following a series of measurements during which that material has been used as a refrigerant.

## 2. Adiabatic shield control

Control of the temperature of the adiabatic shield relative to that of the can may be maintained either manually, as discussed by Skochdopole

(1954), or semi-automatically. The semi-automatic system used in this research consists of four individual control channels, one for each of the shield components, including the RING. Each of the three main channels contains a Leeds and Northrup "M-line" deviation amplifier (Model #177258), an "M-line" controller (Model #177251), and a Kepco voltage-regulated D.C. power supply (Model #ABC 200M). The RING channel (Model #687293) contains similar components of Honeywell manufacture and has the capability that the deviation amplifier "zero" may be offset by any desired amount up to  $\pm 45$  millivolts. The power supply unit in the fourth channel uses a silicon-controlled rectifier power supply (Model #R7170A). Finally, the output voltage of the MASH deviation amplifier is monitored with a strip-chart recorder. This gives a continuous record of the quality of the shield control throughout the course of a run, since the behavior of the other components closely follows that of the MASH.

The deviation amplifier is a high-gain, ( $10^6$  referred to the input), low-noise D.C. amplifier designed to reliably detect and amplify signals in the microvolt range, as from the shield-can difference thermopiles. The sensitivity of the instruments used here is of the order of  $\pm 0.2$  microvolt. The lower detection limit imposed by the presence of extraneous thermal e.m.f.'s in the thermocouple circuits is probably of the order of 0.1 microvolt. The output voltages from the deviation amplifiers are developed across the input terminals of the controllers. Similarly, the output voltages of the controllers are developed across the input terminals of the Kepco units, and determine the power developed in the shield heaters.

The controller units are amplifiers, the feedback circuits of which are designed to perform various functions such as proportioning and reset

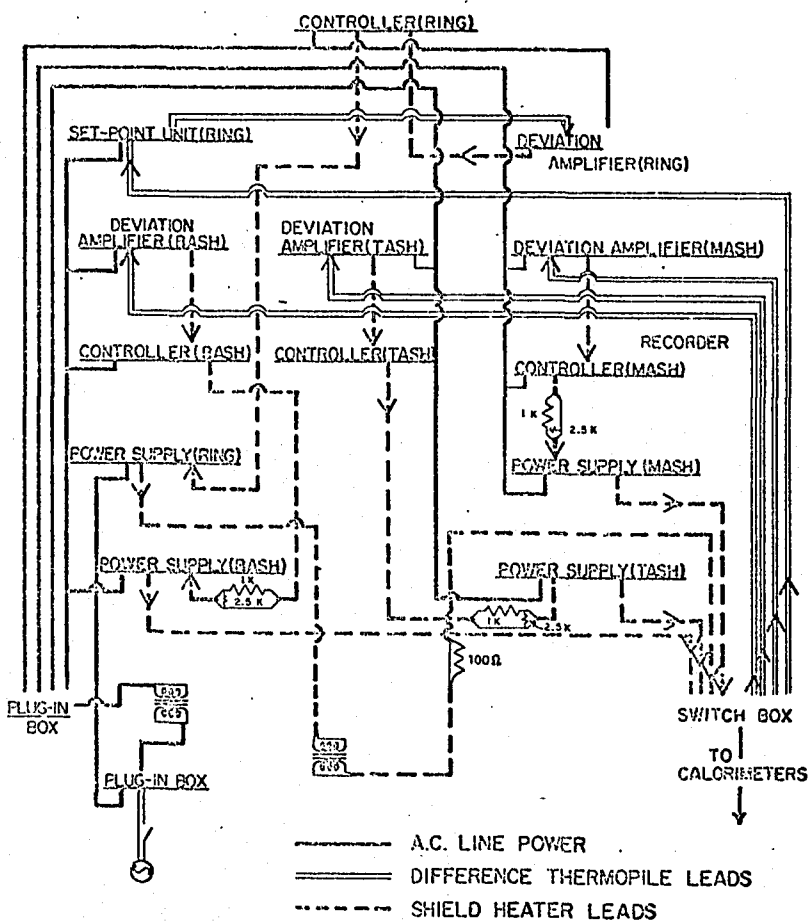
control. Proportioning control involves effectively, varying the output of the controller amplifier. When adjusted to a relatively "wide proportional band" setting, the controller's response to an offbalance voltage from the deviation amplifier is to partially cancel the effect of that voltage. Therefore, in order for the power supply unit to send a given current through the shield heater, an even larger offbalance voltage is required from the deviation amplifier. This results in the temperature difference between the shield and the can varying over a relatively wide range. When the controller is adjusted to a relatively narrow proportional band setting, the power supply unit "sees" the full effect of the offbalance voltage from the deviation amplifier and accordingly sends a relatively larger current through the heater. The temperature difference then varies over a much narrower range. Obviously the second condition is preferable. However, in order for it to exist, the response time of the shield must be approximately equal to that of the control system. For example, at temperatures below about  $15^{\circ}\text{K}$  the relatively low heat capacity of the shield causes the system to over-react. Even on a narrow proportional band setting, the control system requires a finite time to respond to a sudden change in the shield temperature i.e., as on being heated by the control system. The result is that the shield strongly overheats relative to the can. Similarly at any temperature, if the difference thermocouples and/or heaters are not in sufficiently good thermal contact with their respective components, the shield behaves sluggishly compared to the control system. The function of reset control is to gradually attenuate the proportioning feedback voltage. The length of the attenuation cycle is governed by the time constant of the reset circuit, which is adjustable.

Figure 4 is the wiring diagram for the adiabatic shield control system. Electrical leads from the calorimeter enter at the lower right of the figure. Those from the A.C. line enter at the lower left. The difference thermocouple leads are electrically shielded, as are the leads between the deviation amplifiers and the controllers. All of these shields are connected at a common point, to a good earth ground. The 1K and 2.5K resistors between the controllers and the Kepco power supplies are necessary to minimize a "base" heater current which is inherent in the system. Their presence reduces the zero-level power developed in each of the adiabatic shield heaters from about 5 milliwatts, which is significant, to about  $10^{-3}$  microwatts, which is not. The leads between the power supplies and the heaters are fused at 125 milliamps. Between the RING power supply and its heater is interposed an isolating transformer. This serves to protect the silicon controlled rectifier from a possible short circuit at the RING heater.

In practice, the controller settings are determined by the behavior of the control system. This in turn, for a properly designed shield assembly, is largely a function of the temperature range in which measurements are being made. In the range  $4^{\circ}\text{K} < T \leq 7^{\circ}\text{K}$  there is a strong tendency for the system to over-react as noted above. Quite acceptable control can be maintained however, with "wide" proportional band settings and no reset attenuation. In the range  $7^{\circ}\text{K} \leq T \leq 30^{\circ}\text{K}$  the temperature of the shield follows that of the sample both at the beginning and at the end of a heating period. Shield control to within  $\pm 0.5$  microvolts is maintained in this range by the gradual "narrowing" of the proportional band and the addition of reset control with increasing temperature. The poorest control is observed in the

Figure 4. Wiring diagram of the semi-automatic adiabatic shield control system





range  $30^{\circ}\text{K} \leq T \leq 80^{\circ}\text{K}$ . This region is characterized by the shield temperature being out of step with that of the can, both at the start and at the end of a heating period, by about 1 microvolt. The specific behavior is complex and depends upon the controller dial settings, the nature of the refrigerant in the helium reservoir, the RING-MASH temperature difference, the sample heating rate, and the thermal conductivity within the calorimeter can. This last depends upon the thermal contact between the sample and the calorimeter can. Within this temperature range, the quality of the control may be maintained to well within acceptable limits (i.e., such that the "hot" and "cold" deviations average to zero over the measurement of a data point, and remain less than a microvolt in magnitude) by the partial use of manual control. In the range  $80^{\circ}\text{K} \leq T \leq 300^{\circ}\text{K}$  the best control is observed. The control system accepts relatively "narrow" proportional bands and high reset attenuation rates. The temperature deviations average to zero to within  $\pm 0.2$  microvolt. With the thermopiles previously described, the sensitivity of the system is such that the rate of heat transfer between the can and the surroundings per unit thermopile offbalance is approximately  $10 \text{ millijoules minute}^{-1} \text{ microvolt}^{-1}$ .

### 3. Thermometer

As originally conceived, the calorimeter was to have included two thermometers. The need to minimize the mass of the addenda, relative to that of the sample, required them to be no heavier totally than a single thermometer of the type normally used. One of them, a germanium resistor, would have been useful in the measurement of temperature differences below  $15^{\circ}\text{K}$ . The other was to have been a miniature platinum resistor, to be used

in the range  $10^{\circ}\text{K} \leq T \leq 300^{\circ}\text{K}$ . At the time the thermometers were obtained, only three examples of the miniature platinum resistor were available. These were all made by the Minco Products Company. Gehring and Gerstein (1967) had studied the effect of thermal shocking to liquid helium temperatures upon the reproducibility of the resistance of these thermometers at the triple point of water. On the basis of their results it was felt that, in spite of a peculiarity in the construction of the thermometers (to be discussed later) they would be suitable for calorimetry. Accordingly, an attempt was made to calibrate the Minco thermometer (serial #42) in the temperature range of interest.

The Minco thermometer and an L&N platinum thermometer (serial #1549568), to be used as a standard, were placed in machined holes in close proximity in an approximately one kilogram copper block. Aprizon-T grease was used to provide thermal contact between the thermometers and the block. This assembly was suspended in place of the can, inside the adiabatic shield, and the calorimeter was used as a calibrating device. The calibrating procedure involved maintaining the temperature drifts at such a value that any two adjacent temperature measurements did not deviate by more than  $10^{-3}$  degrees. Two sets of six consecutive measurements were made of the Minco temperature, and each set was bracketed by a similar set of measurements on the L&N instrument. Each grouping of five sets thus measured constituted a calibration point. Such points were determined at five degree intervals in the range  $20^{\circ}\text{K} \leq T \leq 90^{\circ}\text{K}$ , and at ten degree intervals thereafter.

The smoothness of the temperature dependence of the resistance of a thermometer is of major importance in calorimetry. A difference function of the form:

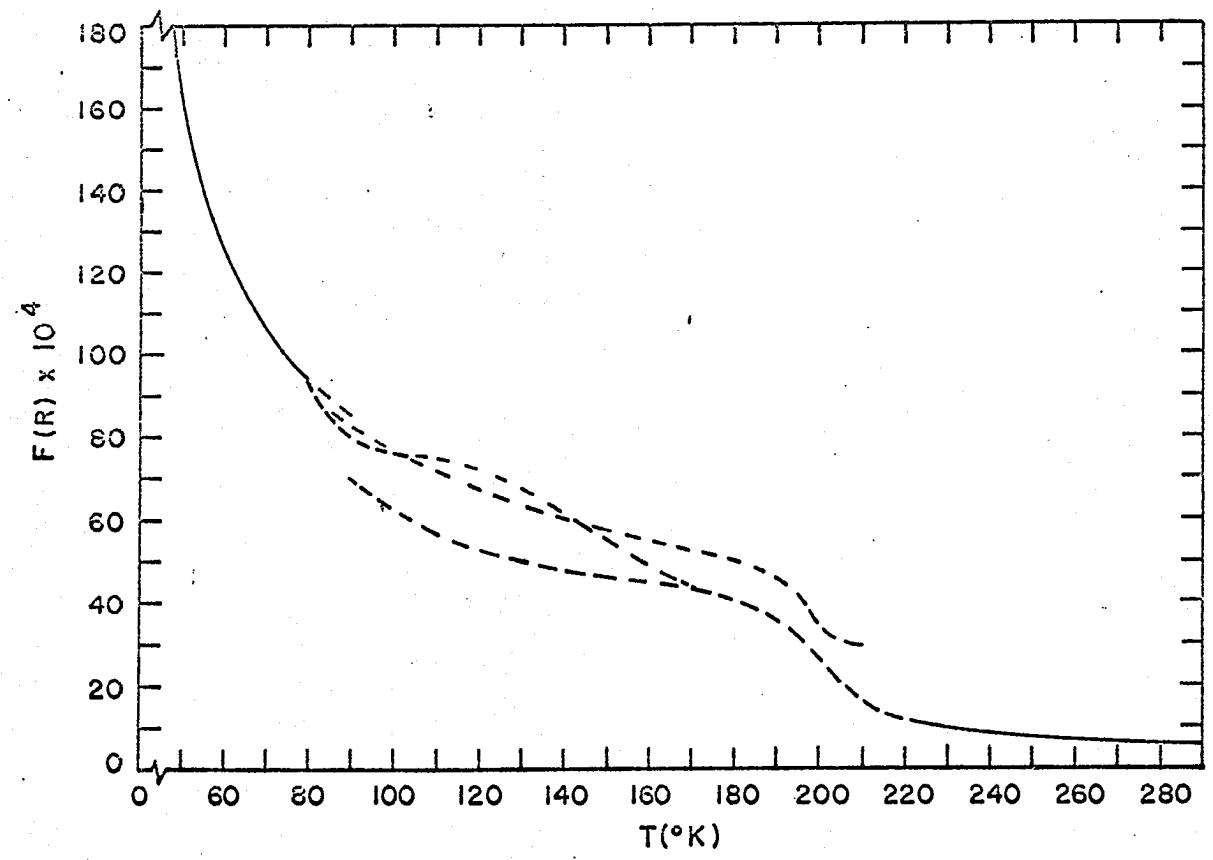
$$F(R) = \frac{(R_{PT})_T / (R_{PT})_{T'} - (R_{ST})_T / (R_{ST})_{T'}}{(R_{PT})_T / (R_{PT})_{T'}} \quad (5)$$

was chosen to study this property for the Minco instrument. The subscripts refer to the Minco thermometer (PT), some standard (ST), whose resistance is known to vary smoothly with temperature, a fixed temperature ( $T'$ ), such as  $273^{\circ}\text{K}$ , and some variable temperature ( $T$ ). The standard was chosen to be a hypothetical platinum resistor of ideal purity. The resistance ratio for such a resistor has been determined as a function of temperature by Berry (1963).

Figure 5 is a plot of  $F(R)$  as a function of temperature in the range  $50^{\circ}\text{K} \leq T \leq 290^{\circ}\text{K}$ . Each of the dashed curves represents a separate attempt to characterize the region. The behavior of the Minco thermometer is strongly discontinuous and non-reproducible over an appreciable portion of the temperature range of interest. This behavior is evidently due to the peculiar nature of the construction of the thermometer.

Such an instrument normally consists of a coil of strain-free platinum wire, wound on a mica form and joined to two electrical leads at each of its ends. These four leads then extend through a vacuum seal to the outside of the thermometer case. The construction of Minco #42 differs in that a length of Kovar wire connects one end of the platinum to the external leads. Thus, the Kovar is effectively a part of the temperature-sensing element. Appreciable strains probably develop within the seal and thus result in the unpredictable behavior of the thermometer. Since all of the available miniature platinum thermometers had the same design fault, they were useless

Figure 5. Difference function for studying the smoothness of the temperature dependence of the Minco thermometer resistance



for calorimetry. This made it necessary to eliminate the germanium resistor also, because of the size of the other available commercial platinum units.

The thermometer actually used for the heat capacity measurements was the L&M instrument, employed in the Minco calibration. Prior to its being installed in the heater/thermometer assembly discussed earlier, determinations were made of its water-triple-point resistance. The results of these determinations, in terms of the ratio of the resistances of 25 and 100 ohm standard resistors, were compared to the results from the previous measurement of another N.B.S. calibrated thermometer. The ratios agreed to within better than 0.01%. This measurement served as a check on the stability of the thermometer over a period of time, and as a guarantee that it had not suffered from mechanical or thermal shock since it had been calibrated.

#### 4. Potentiometer

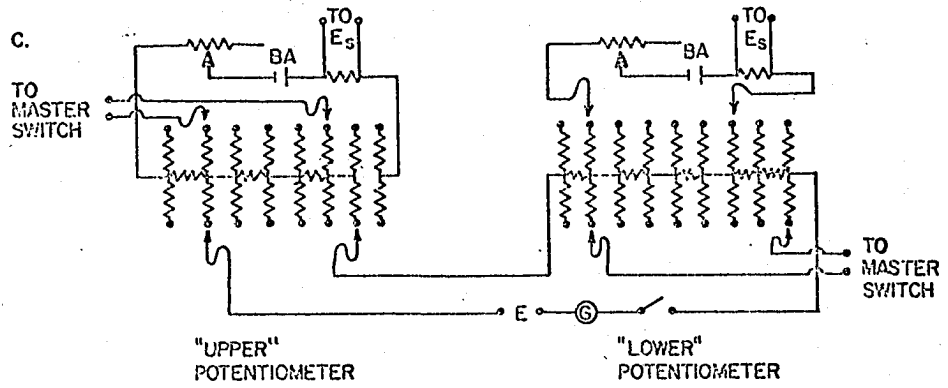
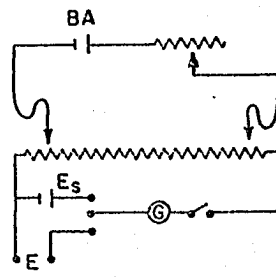
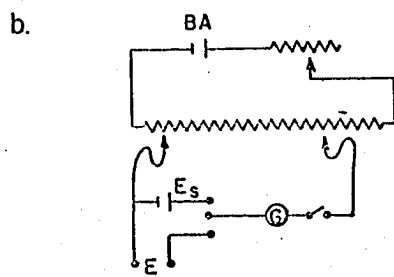
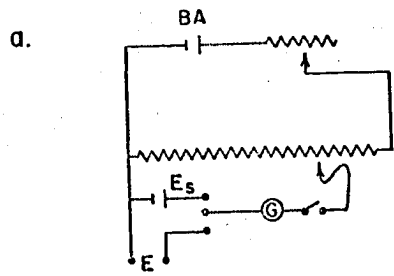
Skochdopole (1954) has described the circuitry which interconnects the thermometer, the sample heater, their respective power sources and regulating devices, and the potentiometer. Therefore, this information will not be discussed in detail. A one or four milliamp current, constant to the order of a part in  $10^5$ , is supplied to the thermometer by three Willard batteries. The choice of the magnitude of the current is at the option of the experimenter. The current through the thermometer and the voltage drop across it are measured with a potentiometer of a type suggested by White (1914a, 1914b) and designed and built by the Leeds and Northrup Company.

In general it is desirable for a potentiometric measuring circuit to have certain characteristics such as: (a) the existence of no undetermined resistances in the measuring dials, (b) the occurrence of no change in the resistance in series with the battery (to within one part in  $10^5$ ) due to a change in the dial settings, (c) a constant (to within 0.5%) resistance in the galvanometer circuit, (d) thermal e.m.f.'s in the galvanometer circuit which are relatively small and insensitive to the measuring dial settings and (e) a potentiometer resistance which is optimal with respect to its effect on the galvanometer sensitivity. In this work it is necessary to measure two different voltages of approximately equal magnitude on a single set of potentiometer resistors. These voltages may be, for example, the potential drop across the thermometer and that across a standard resistor in the thermometer current circuit. Moreover, these measurements are made alternately at half-minute intervals. Obviously, in order to avoid the great opportunity for error involved in changing the settings of each of four dials twice a minute, it is desirable to be able to use the single motion of a double-throw switch to accomplish the change. The design of the White double potentiometer is such that it displays the stated characteristics plus several others which, taken together, make it quite well suited to the purpose at hand.

Figure 6 illustrates the development of some of the principal features of this instrument. Part (a) represents a simple potentiometer circuit. The symbols stand for the potentiometer battery (BA), the unknown voltage ( $e$ ), and the standard cell ( $e_s$ ). Two alternative ways of arranging the measuring dials are shown in part (b). In the arrangement on the left, the battery circuit is not affected by the contact resistance, but the effect of



Figure 6. Some of the principal features of the White double potentiometer



thermal e.m.f.'s will be seen in the galvanometer circuit. In the arrangement on the right, the contacts are in the battery circuit, where the thermal e.m.f.'s are in series with the relatively large battery voltage, hence negligible. The contact resistance will, however, effect the battery current. For this reason, the switches on the right must be of a high quality relative to those on the left. In either arrangement, it is necessary to add compensating resistors so that the resistance in the circuit containing the contacts remains constant for any dial setting. These are shown in part (c). Also in part (c), it has been indicated how two potentiometers of the type shown in part (b) are joined to form a "combination" potentiometer. A "combination" potentiometer becomes a "double" potentiometer when provisions are made for: (1) two independent sets of dials upon which the value of two independent voltages may be set and (2) a way of switching the potentiometer(s) between them. The diagram suggests how these two requirements are met. The galvanometer and the potentiometer(s) are exchanged between the two voltages to be measured by means of a six-pole, two-throw master switch, which is not shown. The connections joining the measuring dials (e) and the galvanometer are actually routed through this switch, rather than as shown in the figure. The complexity of the circuits is such that the essential features tend to become lost in diagrams of greater detail. Also, such detail is readily available in the original papers by White (1914a, 1914b) and in the L&N publications concerning the White potentiometers. Several advantages exist for the potentiometer arrangement in part (c). The lower potentiometer may have a battery circuit resistance of the order of  $2 \times 10^4$  ohms without affecting the galvanometer sensitivity. The lower dials thus tend not to cause problems of contact

resistance. With those dials placed in the battery circuit, thermal e.m.f.'s are not seen in the galvanometer circuit. The upper potentiometer, across which 99,000 out of 99,990 microvolts may be balanced, is then of a design which is more reliable from the standpoint of the elimination of contact resistance from the battery circuit. The presence of two potentiometers allows one set of resistors to be characterized in terms of the other set. The entire double potentiometer can then be made to be internally self-consistent. Further, the measurement of two voltages on a single set of potentiometer resistors allows the errors in the resistors to effectively cancel in the ratio of the voltages. A practical advantage of this instrument is the simplicity of its design as compared to that of an electronic voltage measuring device of approximately the same sensitivity. This simplicity is important for the relative directness with which difficulties, when they occur, may be located, understood, and corrected.

Two White double potentiometers were used during the course of this work. The first, having the L&N serial #777877, eventually became worn out from the cumulative effects of approximately twenty years service. The principal problems with this instrument occurred in the master switch. By the time the heat capacity measurements of the final sample (the Lu salt) were begun, it had become necessary to dismantle and clean this switch prior to each day's run. At that time, another instrument had become available. This one, having an L&N serial #770299 was auto-calibrated and used to finish the set of heat capacity measurements. Auto-calibration is the procedure whereby the double potentiometer is made internally self-consistent, as mentioned above.

## C. Procedures

Westrum, et al. (1968) have published a detailed review of current practice in adiabatic low-temperature calorimetry. Skochdopole (1954) and Gerstein (1960) have described the techniques used in the Ames Laboratory during the 1950's. Although procedures often are changed to meet varying requirements, the measurements in this work were carried out in much the manner described by these authors. The only significant differences arose from the use of semi-automatic adiabatic shield control and from the need for special care in preparing the hydrated samples. Each of these topics has been discussed in an earlier section. Because of the essential similarity of the present techniques to those of previous authors, some of what follows is repetitious. However, it is felt that a brief description of the experimental procedures used in this work will contribute to the continuity of the entire discussion.

A carefully weighed quantity of the sample plus a quantity of dry helium at 2 cm Hg pressure and 298<sup>0</sup>K are sealed into the calorimeter can and the seal is leak-tested. In the case of a hydrate, the equilibrium vapor pressure of water over the sample is measured and adjusted if necessary, prior to the sealing of the can. The can is inserted into the calorimeter, as described in the previous section, and the heater/thermometer assembly and thermocouple junctions attached. All of the components within the adiabatic shield, including the electrical leads but excluding the sample, are considered to be "addenda." In order to avoid measuring the heat capacity of the addenda for each sample measured, every effort is made to keep the addenda constant. In practical terms, this means

continuously monitoring the weight of the can, the solder, the thermal contact grease, and any other part of the addenda that might change as a result of handling.

The heat capacity (vide infra) associated with the mean temperature of the interval  $[T_1, T_2]$  is (Westrum, et al., 1968).

$$C = \frac{Q}{T_2 - T_1} \quad (6)$$

For the system consisting of sample plus addenda,  $C$  is determined between any two temperatures by introducing heat in the form of a measured amount of electrical energy and observing the resultant temperature change. One such determination constitutes the measurement of one data point. During a determination, the system is thermally isolated from its surroundings by the calorimeter, in particular the vacuum system, and by the adiabatic shield, which is kept at the same temperature as the surface of the can. In general, adiabatic conditions are not perfectly maintained because of: (1) the existence of temperature gradients along the leads and along the shield and can surfaces, (2) extraneous thermal e.m.f.'s in the shield control thermocouple circuits, which result in non-zero temperature differences between the can and the shield, (3) self-heating of the thermometer, which is essentially constant over a series of samples and is therefore a part of the addenda, and (4) heat introduced to the can via the winch line, a constant in the same sense. These imperfections appear as regular variations in the sample temperature with time. These temperature "drifts" are measured and are used in the determination of  $T_1$  and  $T_2$ , the "initial" and "final" temperatures at the middle of the heating period.

Specifically, the voltage drops across the thermometer and across a standard resistor in series with it are observed typically for six minutes prior to the introduction of heat, and again for six minutes after the return of the system to a steady state, following heating. The "final" drift of a given data point is the "initial" drift of the following point. Temperature differences are observed to the order of 0.001 degree, while temperatures may be known to 0.01 degree.

The electrical energy introduced to the system during a heating period is measured by observing the voltage drop across a known fraction of a resistor in parallel with the sample heater and the voltage drop across a known resistor in series with the heater. It has been shown (Skochdopole, 1954) that heating measurements need be made only during the three minutes bracketing the center of the heating period. That is, comparisons have been made between the heat input values determined from power measurements made over the central portion of the heating period and those determined from measurements made over the entire period. These comparisons have shown that the former method results in an accuracy in determining the heat input which is at least an order of magnitude better than our ability to measure  $\Delta T$ .

Calculation of the heat introduced to the system and of the initial and final temperatures of a heating period, for which the raw data are the voltage measurements and the known resistance values, are made on the IBM 360 computer. The program for performing these calculations was written in 1963 by M. K. Rhyne of the Ames Laboratory Computer Services Group. As an example of the data treatment, the computer converts the thermometer voltage and resistance data to temperatures and least-squares fits the

temperature-time points for a given temperature drift to a straight line. If the mean deviation of the data from the line is greater than that which would lead to an error in  $\Delta T$  of one half the expected experimental error, the machine may least-squares fit the drift as a function of temperature to the two drifts on either side of the drift in question. The performance of this last operation is at the discretion of the experimenter. The temperatures at the midpoint of a heating period are determined on the basis of the initial and final drifts and the time between midpoints. The "mean" heat capacity (equation 6) of the sample at a given temperature is then calculated from the measured heat input and temperature change, the previously determined addenda heat capacity, and the known weight, corrected to vacuum, of the sample.

To the extent that the heat capacity is linear in temperature over a sufficiently small temperature interval, the mean heat capacity is approximately equal to the true heat capacity:

$$C_p = \left. \frac{dH}{dT} \right|_p = \lim_{\Delta T \rightarrow 0} \left. \frac{Q}{\Delta T} \right|_p \quad (7)$$

(Here constant pressure, to which the experimental conditions provide a sufficiently good approximation, has been specified.) Methods exist (Mcstrum, et al., 1968) for the correction of the mean heat capacities for the "curvature" effect, and are frequently applied, especially in regions of relatively rapid change in the slope of the heat capacity as a function of temperature. One of the criteria for choosing a given sample heating current, prior to the start of a run, is the desired value of  $\Delta T$ . For regions of the heat capacity curve in which there is no anomalous behavior,



and for which  $C_p$  varies sufficiently slowly with temperature,  $\Delta T$  is routinely chosen to be of the order of 10% or less of  $T$ . For the present measurements,  $\Delta T$  was seldom larger than 15 degrees at the highest temperatures reported.

The computer-generated heat capacities are plotted as a function of temperature on one meter wide graph paper and the smoothed curve values are obtained from a spline-fit curve. Graphical tests are routinely applied to the data to determine whether curvature corrections are necessary. In this work it was always the case that such corrections were not necessary. The smoothed curve typically fitted the data to within  $\pm 0.1\%$  in the range  $50^\circ\text{K} \leq T \leq 230^\circ\text{K}$ . Above  $230^\circ\text{K}$  there were usually a number of experimental points deviating from the smoothed curve by  $\pm 0.15\%$  or more. The precision below  $30^\circ\text{K}$  will be discussed in connection with the benzoic acid results. The thermodynamic functions, equations 8, 9, and 10 were obtained by computerized graphical integration of the smoothed curve results.

$$S_T^0 = \int_0^T C_p / T \, dT \quad (8)$$

$$H_T^0 - H_0^0 = \int_0^T C_p \, dT \quad (9)$$

$$\frac{F_T^0 - H_0^0}{T} = \frac{H_T^0 - H_0^0}{T} - S_T^0 \quad (10)$$

## IV. RESULTS

## A. Heat Capacities

1. Addenda

The calorimeter can used in these measurements weighed approximately 134 grams. The Bi/Cd solder and the Ag exchange gas port added another 3 grams. The heater/thermometer assembly weighed approximately 16 grams. Thus the weight of the addenda was of the order of 153 grams, exclusive of thermal contact grease, bolts, wires, and adhesive. The average sample weights were of the order of 100 grams. The addenda contributed somewhat more than one third of the total heat capacity at 300<sup>0</sup>K. The can and the heater/thermometer shell were gold-plated.

Table 3 lists the smoothed curve values of  $Q/\Delta T$  as a function of  $T$  for the addenda. These values were determined from two sets of measurements made over the entire temperature range. The precision over both sets of measurements was  $\pm 0.1\%$  of  $Q/\Delta T$ , except as previously noted. The precision of the data within a single set of measurements was of the order of several hundredths of a percent. This difference between the precision of the individual data sets and the over-all precision is possibly due to the anomalous behavior of the heat capacity of Apiezon-T grease in the temperature region above 200<sup>0</sup>K, (Westrum et al., 1967). The addenda contained approximately 70 milligrams of this material, as noted above. The difference was found to be not related to the magnitude of the sample heating current, the behavior of the adiabatic shield control, variations in the cleanliness of the measuring circuit switches, or variations in the addenda, aside from the grease. The reproducibility of the thermometer is such as

Table 3. Experimental values of  $Q/\Delta T$  for the addenda (joules deg.<sup>-1</sup>)

$T(^{\circ}\text{K})$	$Q/\Delta T$	$T(^{\circ}\text{K})$	$Q/\Delta T$
0	0.000	45	12.081
1	0.002	46	12.649
2	0.004	47	13.228
3	0.008	48	13.805
4	0.016	49	14.387
5	0.027	50	14.965
6	0.044	51	15.542
7	0.067	52	16.124
8	0.097	53	16.704
9	0.136	54	17.280
10	0.182	55	17.855
11	0.237	56	18.422
12	0.300	57	18.990
13	0.375	58	19.556
14	0.465	59	20.116
15	0.569	60	20.675
16	0.688	61	21.230
17	0.821	62	21.778
18	0.971	63	22.321
19	1.137	64	22.858
20	1.325	65	23.392
21	1.535	66	23.916
22	1.763	67	24.424
23	2.016	68	24.932
24	2.288	69	25.422
25	2.583	70	25.908
26	2.904	71	26.381
27	3.242	72	26.851
28	3.601	73	27.317
29	3.982	74	27.784
30	4.381	75	28.250
31	4.800	76	28.705
32	5.242	77	29.160
33	5.698	78	29.608
34	6.169	79	30.053
35	6.650	80	30.484
36	7.148	81	30.918
37	7.662	82	31.346
38	8.190	83	31.765
39	8.721	84	32.174
40	9.270	85	32.576
41	9.817	86	32.970
42	10.375	87	33.355
43	10.936	88	33.737
44	11.509	89	34.100

Table 3. (Continued)

T(°K)	Q/ΔT	T(°K)	Q/ΔT
90	34.459	185	51.776
91	34.803	190	52.175
92	35.147	195	52.549
93	35.483	200	52.909
94	35.808	205	53.257
95	36.133	210	53.583
96	36.448	215	53.889
97	36.762	220	54.186
98	37.074	225	54.467
99	37.380	230	54.741
100	37.679	235	54.997
105	39.117	240	55.245
110	40.450	245	55.489
115	41.664	250	55.727
120	42.799	255	55.952
125	43.848	260	56.168
130	44.821	265	56.380
135	45.725	270	56.584
140	46.560	275	56.778
145	47.324	280	56.959
150	48.026	285	57.137
155	48.685	290	57.307
160	49.293	295	57.465
165	49.863	300	57.618
170	50.390	305	57.762
175	50.890	310	57.902
180	51.348	315	58.029

to be unrelated to observed effect. Multiple measurements of the heat capacity of a given sample have confirmed the general  $\pm 0.1\%$  reproducibility of the data.

## 2. Benzoic acid

The heat capacity of about 0.48 moles of 1949 Calorimetry Conference standard benzoic acid was measured as a check on the operation of the calorimeter. The experimental values of  $Q/\Delta T$  and of  $Q/\Delta R$  are listed in

Table 4. The columns labeled "Block Number," so-called by local convention, list the numbers of the original data sheets.

A bump due to a discontinuity in the thermometer table had been observed in the heat capacity of the addenda at about 10<sup>0</sup>K. The results of the benzoic acid measurements were used as a guide, because of a higher density of data points in this temperature region, to the smoothing of the thermometer table. Essentially the process consisted of varying both the magnitude and the slope of the tabulated resistance-temperature function in such a way as to remove the calculated bumps in the benzoic acid and addenda heat capacities.

Figure 7 is the plot of a difference function between the benzoic acid data reported here and those reported by Ginnings and Furukawa (1953) and by Clay and Staveley (1966). The latter authors claim a ±1% accuracy in their results over the temperature range from 10<sup>0</sup>K to 80<sup>0</sup>K using germanium thermometry. The precision of the present measurements is as indicated in the figure. Below about 50<sup>0</sup>K the precision deteriorates rapidly with decreasing temperature because of the decreasing sensitivity of the platinum thermometer. At 20, 12, 10 and 5<sup>0</sup>K the precision is of the order of ±0.5, ±2, ±5 and ±20% respectively.

### 3. GdCl<sub>3</sub>·6H<sub>2</sub>O

The crystals were prepared as discussed in the previous chapter. Prior to the loading of the can, the crystals were crushed so that all of a representative sampling would pass on 80 mesh sieve and 50% would pass a 100 mesh sieve (0.18 and 0.15 mm respectively). This procedure was also applied to the other three salts. The quantity of GdCl<sub>3</sub>·6H<sub>2</sub>O upon which

Table 4. Experimental values of  $Q/\Delta T$  for benzoic acid (joules deg.<sup>-1</sup>)

Block no.	$T_{ave}$ (°K)	Q	$Q/\Delta T$	$\Delta R$	$Q/\Delta R$	$R_{ave}$
394	6.181	0.385	0.261	-	-	-
411	6.236	0.073	0.290	-	-	-
412	6.557	0.097	0.328	-	-	-
413	6.901	0.139	0.379	-	-	-
414	7.402	0.247	0.443	-	-	-
395	7.478	0.488	0.462	-	-	-
415	7.883	0.247	0.559	-	-	-
416	8.300	0.247	0.644	-	-	-
396	8.437	0.643	0.697	-	-	-
417	8.638	0.256	0.779	-	-	-
418	8.978	0.276	0.849	-	-	-
397	9.272	0.733	0.970	-	-	-
419	9.281	0.294	0.950	-	-	-
420	9.580	0.303	1.035	-	-	-
421	9.847	0.315	1.139	-	-	-
398	9.999	0.850	1.229	-	-	-
422	10.112	0.339	1.216	-	-	-
423	10.401	0.412	1.303	-	-	-
424	10.702	0.443	1.418	-	-	-
399	10.717	1.092	1.448	0.0023	483.186	0.0224
425	11.049	0.585	1.554	0.0015	382.353	0.0236
426	11.442	0.659	1.656	0.0011	621.698	0.0249
400	11.531	1.498	1.762	0.0030	491.148	0.0251
427	11.890	0.951	1.864	0.0020	463.902	0.0264
401	12.417	1.936	2.163	0.0041	475.676	0.0287
428	12.465	1.353	2.145	0.0029	471.429	0.0289
402	13.434	3.179	2.874	0.0064	495.171	0.0340
403	14.944	5.173	3.405	0.0122	424.016	0.0447
404	16.434	6.258	4.292	0.0156	401.795	0.0586
405	17.984	8.615	5.264	0.0228	377.851	0.0778
430	19.668	3.185	6.418	0.0089	359.887	0.1038
406	19.732	12.047	6.469	0.0336	358.542	0.1060
431	21.288	20.904	7.609	0.0607	344.496	0.1385
407	21.724	16.843	7.946	0.0493	341.643	0.1474
408	24.009	23.851	9.755	0.0730	326.726	0.2086
432	24.068	27.582	9.800	0.0845	326.414	0.2111
433	27.016	37.935	12.299	0.1203	315.607	0.3134
434	30.490	59.686	15.436	0.1925	310.057	0.4698
435	34.131	64.557	18.889	0.2076	310.968	0.6698
436	37.528	74.786	22.153	0.2324	321.799	0.8937
437	41.131	98.125	25.612	0.3009	326.105	1.1606
438	45.265	131.325	29.573	0.3858	340.397	1.5038
382	49.313	91.551	33.392	0.2564	357.063	1.8665
383	52.535	134.274	36.320	0.3611	371.847	2.1754

Table 4. (Continued)

Block no.	$T_{ave}$ (°K)	Q	Q/ΔT	ΔR	Q/ΔR	$R_{ave}$
385	57.120	219.928	40.334	0.5479	401.402	2.6402
386	62.599	247.270	44.954	0.5839	423.480	3.2064
387	68.234	283.895	49.279	0.6254	453.941	3.8116
388	74.409	353.223	53.628	0.7241	487.810	4.4864
357	81.188	301.267	58.183	0.5742	524.673	5.2347
358	86.516	336.066	61.508	0.6050	555.481	5.8249
359	92.379	404.576	64.698	0.6935	583.383	6.4774
360	99.342	522.660	68.166	0.8461	617.728	7.2474
361	108.266	735.573	72.288	1.1157	659.293	8.2286
362	119.598	962.347	77.081	1.3582	708.546	9.4657
363	131.737	963.554	81.726	1.2728	757.035	10.7812
364	143.260	964.630	85.730	1.2065	799.528	12.0208
365	151.601	480.386	88.431	0.5797	828.680	12.9140
367	157.364	539.012	90.345	0.6293	856.528	13.5253
368	163.760	628.741	92.319	0.7222	870.591	14.2071
369	172.709	1051.180	94.891	1.1694	898.905	15.1533
370	184.371	1201.896	98.207	1.2850	935.328	16.3809
371	196.769	1276.132	101.620	1.3116	972.958	17.6792
440	206.846	1355.591	104.320	1.3517	1002.879	18.7296
372	210.304	1527.696	105.273	1.5076	1013.330	19.0888
441	220.722	1596.364	108.052	1.5289	1044.126	20.1691
373	224.562	1528.516	109.098	1.4479	1055.678	20.5663
442	235.241	1597.377	111.911	1.4698	1086.799	21.6678
374	238.342	1529.544	112.841	1.3943	1168.099	21.9877
443	249.957	1758.065	115.899	1.5544	1131.025	23.1793
376	254.441	1527.324	117.085	1.3343	1144.663	23.6339
445	264.847	1755.627	119.743	1.4956	1173.861	24.7019
377	267.302	1526.403	120.416	1.2923	1181.152	24.9525
446	279.282	1754.289	123.338	1.4448	1214.209	26.1604
378	279.803	1526.118	123.762	1.2522	1218.749	26.2246
379	292.026	1533.882	126.773	1.2248	1252.353	27.4636
447	293.277	1754.935	126.973	1.3981	1255.228	27.5899
380	303.962	1534.081	129.877	1.1911	1287.953	28.6593

measurements were made was 0.2903 moles.

The experimental values of  $Q/\Delta T$  for  $GdCl_3 \cdot 6H_2O$  are listed in Table 5. The smoothed curve heat capacities and the calculated thermodynamic functions are listed in Tables 9 and 10. Table 9 contains only the lattice

Figure 7. Difference function relating the present and some previously published benzoic acid heat capacities



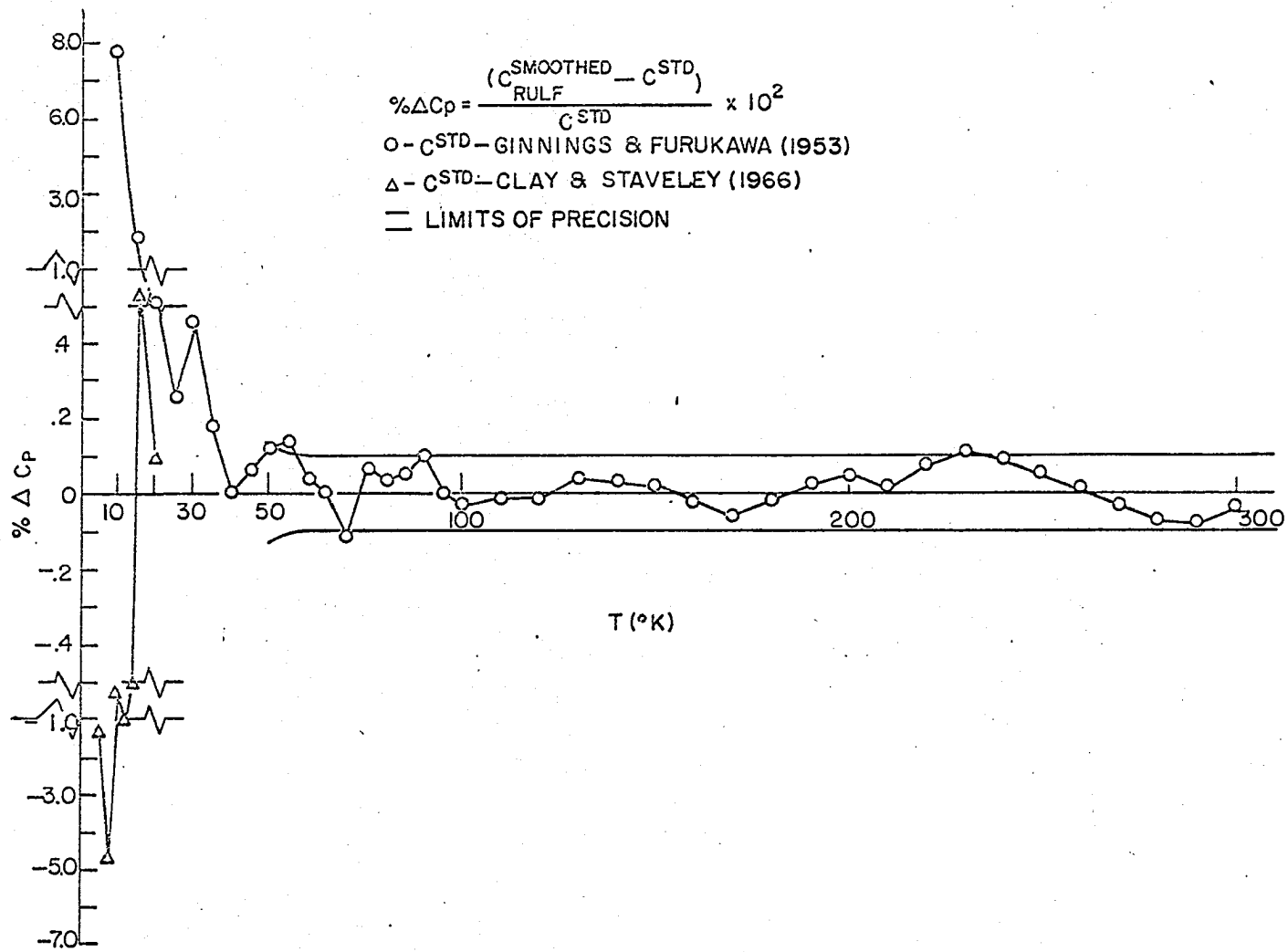


Table 5. Experimental values of  $Q/\Delta T$  for  $GdCl_3 \cdot 6H_2O$  (joules deg.<sup>-1</sup>)

Block no.	$T_{ave}$ (°K)	$Q/\Delta T$
489	4.8706	0.1134
503	5.1611	0.1223
504	6.4354	0.2196
491	7.2192	0.3118
505	7.5877	0.3638
492	8.0691	0.4373
506	8.5203	0.5162
493	8.7449	0.5923
507	9.2995	0.6854
494	9.3686	0.7079
495	10.0026	0.8842
508	10.0801	0.9058
497	10.7435	1.0445
509	10.8519	1.0572
498	11.6022	1.2758
510	11.6995	1.2847
511	12.4822	1.5796
499	12.6487	1.6177
512	13.2476	1.8393
500	13.8997	2.1240
513	14.1407	2.2386
501	15.2973	2.7535
514	15.4297	2.8275
515	17.1538	3.7012
524	17.8442	4.0822
516	18.5806	4.5277
525	19.6798	5.1842
517	19.9475	5.3593
526	21.5211	6.4244
518	21.7465	6.6735
527	23.5582	7.9428
520	23.6806	8.0254
528	25.4041	9.4242
521	25.5673	9.5602
529	27.1141	10.8981
522	27.6115	11.3357
530	29.2521	12.8582
541	29.4779	13.0815
531	31.7841	15.3609
542	32.3966	15.9822
532	34.6416	18.3519
543	35.4672	19.2420
533	37.7150	21.7158
544	38.4569	22.5322

Table 5. (Continued)

Block no.	$T_{ave}$ ( $^{\circ}$ K)	Q/ $\Delta T$
534	40.8577	25.2385
545	41.4364	25.8930
536	43.9020	28.7337
546	44.6551	29.5970
537	46.7703	32.0677
547	48.7110	34.3273
538	49.7717	35.5940
550	52.4673	38.6595
539	53.1580	39.4475
559	53.3279	39.6316
548	53.4614	39.7969
551	56.7442	43.4965
560	58.9624	45.9727
552	61.4050	48.6940
561	65.1650	52.6994
553	66.3525	53.9473
562	71.7433	59.2648
554	71.9178	59.4583
563	78.0808	65.3051
476	82.4385	69.2645
564	86.1924	72.5845
477	92.4151	77.5617
565	96.2634	80.4306
478	102.0440	84.5502
465	109.7291	89.7289
479	111.6564	91.9135
480	121.3601	97.0190
466	121.9713	97.3694
481	131.1454	102.6147
467	133.3543	103.8305
482	141.4130	107.9769
468	144.1049	109.3708
483	152.3276	113.2878
469	155.0613	114.5585
484	163.6530	118.3142
470	166.4227	119.5520
485	175.5392	123.2886
471	178.1720	124.3638
487	187.6172	127.9271
473	191.4716	129.2781
449	199.2222	132.0813
474	205.6173	134.0602
450	209.2581	135.3429
452	220.5283	139.0558

Table 5. (Continued)

Block no.	$T_{ave}$ ( $^{\circ}$ K)	Q/ $\Delta T$
458	229.7831	141.8882
453	233.1807	142.8525
459	244.3041	146.1097
454	247.3823	146.9542
460	258.9868	150.1583
455	261.7669	150.8106
461	273.2742	154.0647
456	275.7859	154.4482
462	287.2051	157.6248
464	301.3355	161.0463

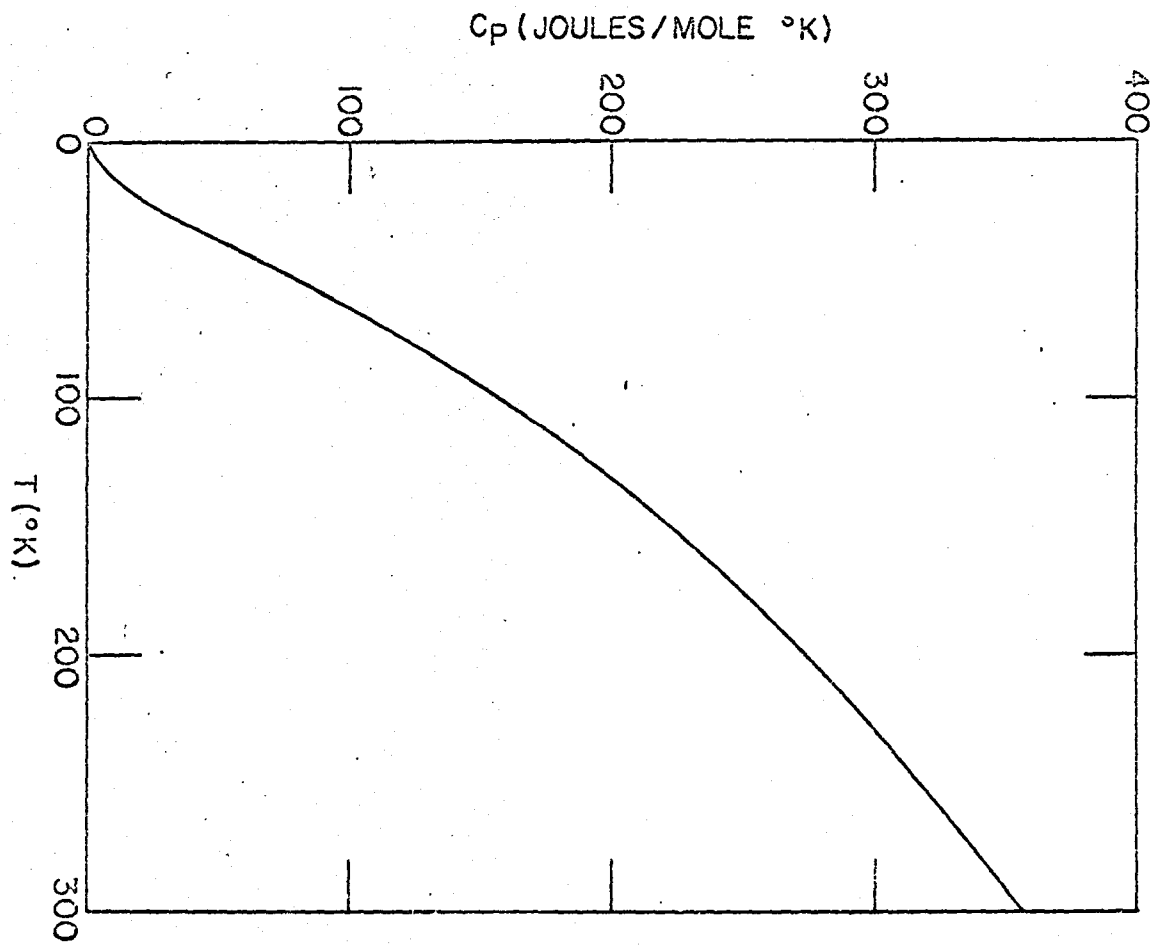
contributions. Table 10 contains the contributions from the lattice and from an approximation to the crystal field split ground state of the  $Gd^{+3}$  ion in this crystal. The topic will be discussed in another section. Figure 8 shows the smoothed curve heat capacity. To within the scale of the figure, the shape of the curve is characteristic of the four samples studied.

#### 4. TbCl<sub>3</sub>·6H<sub>2</sub>O

In order to minimize the uncertainty in the determination of the magnetic contribution to the heat capacity, it is desirable to keep the number of moles of sample constant over a series of samples. The quantity of TbCl<sub>3</sub>·6H<sub>2</sub>O used matched that of the previous sample to within less than  $10^{-4}$  moles.

A standard practice during the heat capacity measurements of the hydrated samples was the examination of the temperature region above 200<sup>o</sup>K for a "water bump" such as that observed by Gerstein (1960). This

Figure 8. Smoothed curve heat capacity of  $\text{GdCl}_3 \cdot 6\text{H}_2\text{O}$



procedure served as a check on the major constituent analysis, that is, on the concentration of the waters of hydration. It has been found that the heat capacity is sensitive to quantities of excess water that constitute several hundredths of a percent of the sample weight.

Table 6 lists the experimental values of  $Q/\Delta T$  for  $TbCl_3 \cdot 6H_2O$ . Table 11 contains the smoothed curve heat capacities and the thermodynamic functions.

#### 5. $HoCl_3 \cdot 6H_2O$

The quantity of this sample used in the heat capacity measurements was 0.2910 moles.

Tables 7 and 12 list the experimental and the smoothed curve values for  $Q/\Delta T$  and  $C_p$  respectively. In the temperature region below  $50^\circ K$  there was generally good agreement between these results and those of Pfeffer (1961a). Figure 9 shows the heat capacity data below  $20^\circ K$ . Some deviation between the present values and those of Pfeffer are evident below  $10^\circ K$ . In particular, the difference is of the order of my experimental error at  $6^\circ K$ . There are several reasons to expect Pfeffer's data to be the more reliable in this temperature region. First, the heat capacity below  $100^\circ K$  is quite insensitive to the occluded water in his crystals. Second, while the sensitivity of a platinum thermometer is relatively low at temperatures of the order of  $10^\circ K$ , that of a carbon thermometer such as used by Pfeffer, is relatively high. Thus his  $\Delta T$  values below  $10^\circ K$  are probably more accurate than mine.

Table 6. Experimental values of  $Q/\Delta T$  for  $TbCl_3 \cdot 6H_2O$  (joules deg.<sup>-1</sup>)

Block no.	$T_{ave}$ (°K)	$Q/\Delta T$
630	4.3883	0.6122 <sup>a</sup>
673	4.5177	0.5451 <sup>a</sup>
631	4.6520	0.5592
674	4.7088	0.6792
675	4.9770	0.7452
632	5.0139	0.7152
676	5.4244	0.7265
633	5.7112	0.7194
677	6.0942	0.7104
609	6.4422	-1.2833 <sup>a</sup>
610	6.5671	0.8481
611	6.9011	0.7723 <sup>a</sup>
678	7.0129	0.7841
612	7.3910	0.8511
635	7.8838	0.8280
613	8.0897	0.8631
679	8.2041	0.9129
614	8.8508	0.9887
636	9.2278	1.0767
680	9.5019	1.1565
615	9.6461	1.1918
637	10.5219	1.3560
617	10.5547	1.3746
681	10.9372	1.4489
618	11.5530	1.6428
638	11.6947	1.6652
619	12.5472	1.9663
640	12.9429	2.1403
620	13.6932	2.4681
641	14.5570	2.8737
621	15.1828	3.1915
642	16.6378	3.9842
622	16.6709	4.0035
623	18.2692	4.9608
643	18.8437	5.3302
624	19.9433	6.0713
645	20.2951	6.3115
625	21.5709	7.2477
646	22.2187	7.7363
626	23.4211	8.7147

<sup>a</sup>Rejected.



Table 6. (Continued)

Block no.	$T_{ave}$ ( $^{\circ}$ K)	Q/ $\Delta$ T
647	24.5825	9.6637
627	25.6125	10.5687
648	27.4799	12.2479
628	28.1598	12.8857
649	30.9101	15.5942
655	32.8676	17.6212
650	34.8314	19.7508
656	35.7290	20.7336
651	39.1721	24.5867
652	43.6623	29.7420
658	44.5986	30.8339
653	48.0231	34.8444
659	49.6577	36.7583
666	52.8253	40.4056
661	55.1377	43.1653
667	57.8555	46.1173
662	61.1232	49.7785
668	62.5501	51.3501
669	67.6077	56.6765
663	68.0649	57.1102
670	73.2341	62.1820
664	75.2686	64.1295
671	79.1144	67.7859
564	80.5355	69.0864
589	80.7539	69.2882
565	87.0058	74.8223
590	88.3203	75.9187
566	93.4708	79.9155
592	95.4771	82.1441
567	100.2223	84.8151
593	105.1677	88.2835
568	107.7205	89.9573
594	115.7554	95.1219
569	116.1796	95.3627
570	125.4167	100.8557
595	127.6975	102.0741
571	135.4274	106.3225
597	138.8457	108.0598
572	146.3526	111.7940
598	150.1279	113.6034
574	157.4741	116.8535
599	161.6456	118.7269
575	168.7498	121.5100
600	173.3766	123.5536

Table 6. (Continued)

Block no.	$T_{ave}$ ( $^{\circ}$ K)	Q/ $\Delta T$
577	180.2457	126.0710
601	185.3618	128.1064
578	191.3097	130.3341
602	196.9456	132.1666
579	202.9331	134.0711
603	209.4063	136.1560
580	215.1342	138.0117
604	223.9135	140.6145
581	228.8054	141.8919
683	234.8792	143.9372
606	239.0796	145.3078
582	243.8414	146.1432
684	249.8458	148.1163
607	253.9391	149.3893
583	258.4392	150.3124
685	264.4146	152.0079
585	272.5034	153.9804
686	278.6248	155.7130
586	286.4124	157.5419
587	300.1072	160.9753

Table 7. Experimental values of Q/ $\Delta T$  for  $\text{HoCl}_3 \cdot 6\text{H}_2\text{O}$  (joules deg. $^{-1}$ )

Block no.	$T_{ave}$ ( $^{\circ}$ K)	Q/ $\Delta T$
772	4.5107	2.1349 <sup>a</sup>
773	4.6683	1.1478
774	5.0103	1.2767
752	5.2824	0.3409 <sup>a</sup>
775	5.3542	1.5055
753	5.4457	0.9498
754	5.6341	1.1378
776	5.9582	1.6103
730	6.0607	0.3634 <sup>a</sup>
731	6.1693	1.4577

<sup>a</sup>Rejected.

Table 7. (Continued)

Block no.	$T_{ave}$ ( $^{\circ}$ K)	Q/ $\Delta T$
755	6.1699	1.5438
732	6.4803	1.8093
777	6.6273	1.6988
733	6.9136	1.7501
756	6.9501	1.8068
778	7.3745	1.9114
734	7.4443	1.8355
757	7.9591	1.9986
735	8.0873	2.0769
779	8.2666	2.1355
736	8.8752	2.2636
758	9.1845	2.3522
780	9.3560	2.2457
737	9.7784	2.5468
781	10.6914	2.5764
759	10.7607	2.6243
738	10.9234	2.6284
739	12.2514	2.9668
760	12.6179	3.0731
740	13.6957	3.4294
761	14.4140	3.5990
741	15.1851	4.0280
763	15.7732	4.2907
742	16.7049	4.7124
764	17.0633	4.8802
743	18.2946	5.5248
765	18.6619	5.7206
744	20.0629	6.5514
766	20.9661	7.1277
745	22.1052	7.8940
767	23.7064	9.0760
746	24.5427	9.7172
768	26.2211	11.0950
747	27.2493	11.9761
748	30.0287	14.5301
783	31.3070	15.7760
770	31.6684	16.1294
749	32.6382	17.1221
784	34.0231	18.5651
750	35.1539	19.7626
785	37.2707	22.0620
795	40.2614	25.3791
786	41.0939	26.3335
796	42.9470	28.4250

Table 7. (Continued)

Block no.	$T_{\text{ave}}$ ( $^{\circ}\text{K}$ )	$Q/\Delta T$
787	45.5282	31.4122
797	46.5202	32.5620
788	50.6098	37.2944
798	51.8367	38.6933
789	56.2994	43.7593
799	58.0247	45.7059
791	62.6961	50.8615
800	64.9377	53.2172
792	69.6077	57.9780
801	70.3728	58.7121
802	73.0470	61.3456
803	75.6161	63.7791
793	76.9023	64.9909
804	78.8030	66.7457
709	85.4625	72.7597
688	88.5134	75.3040
710	92.9918	78.7887
689	95.8739	80.9162
711	101.9617	85.2699
690	104.5801	87.0136
712	112.4147	92.1885
691	115.0994	87.7513
713	123.0132	98.6348
692	126.6077	100.6807
714	132.9929	104.1834
693	137.8940	105.7554
715	143.2465	109.4543
694	148.6067	112.0210
717	154.5308	114.8017
695	159.5642	115.9781
718	165.0663	119.8127
696	170.8065	121.6310
719	177.8392	124.4308
697	182.3048	125.1411
720	189.8694	128.8493
698	194.0886	130.3432
700	199.2954	132.1808
722	201.6693	133.0118
701	211.8236	136.2526
723	217.8547	138.1227
702	224.6003	140.2061
724	233.4810	142.7575
703	238.7911	144.3381
725	249.2179	147.1855

Table 7. (Continued)

Block no.	$T_{ave}$ ( $^{\circ}$ K)	Q/ $\Delta$ T
704	254.8687	148.8181
726	265.6401	151.6689
705	272.6963	153.4328
727	282.1611	155.8262
706	291.0903	158.1034
728	298.2510	159.8611
707	305.8774	161.7753

#### 6. $\text{LuCl}_3 \cdot 6\text{H}_2\text{O}$

Tables 8 and 13 list the experimental and smoothed curve results for this salt. The sample was changed several times because of known or suspected contamination. Only the third sample contributed to the results presented here. This sample consisted of 0.2905 moles of  $\text{LuCl}_3 \cdot 6\text{H}_2\text{O}$ .

Several unusual difficulties were encountered during the measurement of the heat capacity of this salt. The one involving the potentiometer has been discussed in an earlier section. In addition to, but independent of this problem, the heat capacity displayed anomalous behavior in the temperature region above  $275^{\circ}\text{K}$ . The anomaly took the form of a sharply defined bump in the heat capacity curve, extending from about  $279^{\circ}\text{K}$  to beyond  $285^{\circ}\text{K}$ . The heat capacity in the region  $240^{\circ}\text{K}$  to  $300^{\circ}\text{K}$  is shown in Figure 10.

Initial measurements with the third sample, involving  $\Delta T$ 's large compared to the temperature range of the anomaly, suggested the cause to be excess water. In accordance with the procedure developed by Gerstein (1960) for handling such a situation, some water was pumped from the

Figure 9. Heat capacity of  $\text{HoCl}_3 \cdot 6\text{H}_2\text{O}$  in the temperature region below  $20^\circ\text{K}$

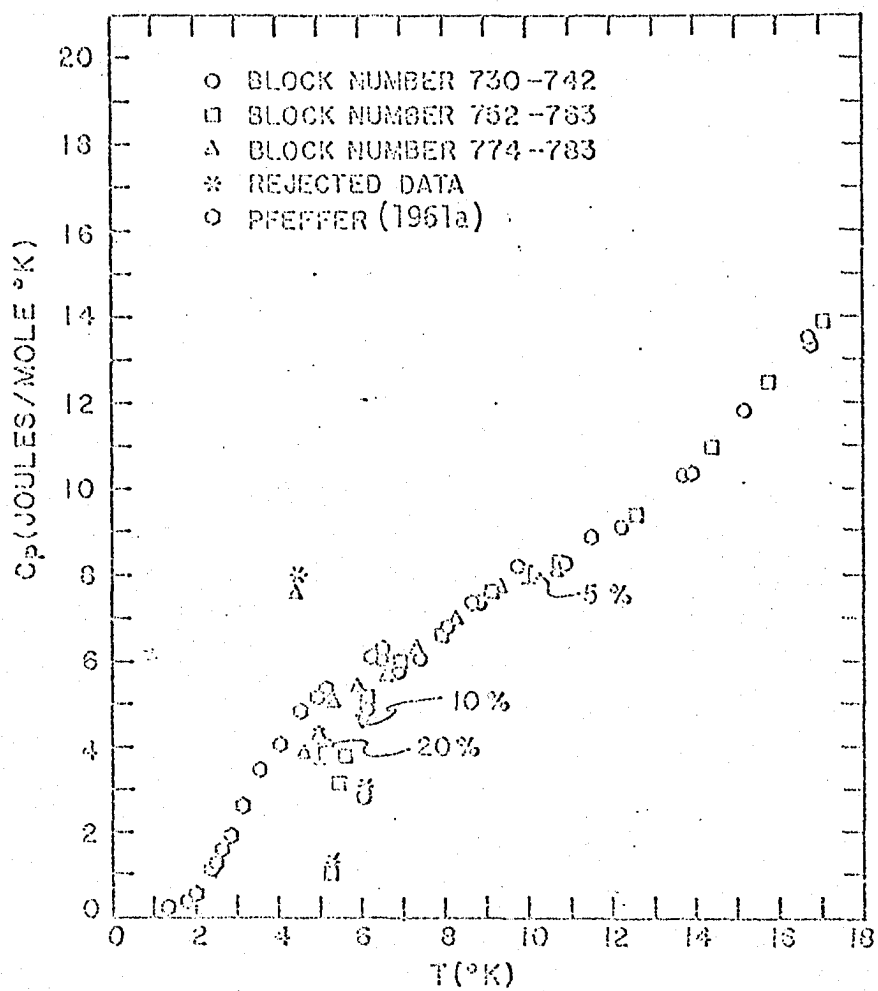


Figure 10. Heat capacity of  $\text{LuCl}_3 \cdot 6\text{H}_2\text{O}$  in the temperature region of the anomaly





crystals, in the can, in an attempt to reduce the size of the bump. Gerstein found that he was able to remove 100 milligrams of water and lower the enthalpy under his "water bump" by about 30 joules. The removal of 25 milligrams of material in the present case caused no significant change in the heat capacity. The data points in Figure 10 designated 3-A were measured before, and those designated 3-B were measured after the pumping.

Further heat capacity measurements, made in order to resolve the shape of the bump, plus chemical analysis of the sample (previously mentioned), established that the bump was most likely not due to occluded water. Additional steps taken to find the cause will be discussed in a later section.

The enthalpy under the bump was estimated to be  $13.8 \pm 1$  joules. This value was obtained from the data of one heating period that covered temperatures ranging from 4 degrees below to 8 degrees above the bump. The area under a smooth curve, extrapolated through the region from the lower temperature data, was subtracted from the measured Q-value of this single heating period. The uncertainty in the enthalpy is due to the difficulty involved in making the extrapolation accurately. The entropy involved in the anomaly is less than  $0.3 \text{ joules mole}^{-1} \text{ deg.}^{-1}$ .

#### B. Magnetic Heat Capacities

The rare earth ions in the Tb and Ho salts studied in this work have ground electronic states which are non-degenerate in the crystalline electric fields within which the ions are situated. The nominally  $2S+1, L_J$  ground states may split into as many as  $(2J+1)$  singly degenerate levels.

Table 8. Experimental values of  $Q/\Delta T$  for  $\text{LuCl}_3 \cdot 6\text{H}_2\text{O}$  (joules deg.<sup>-1</sup>)

Block no.	$T_{\text{ave}}$ (°K)	$Q/\Delta T$
885	5.2159	0.0845
886	5.4621	0.0709
887	5.7276	0.0674
888	6.0198	0.1402
889	6.2143	0.1254
890	6.4708	0.2045
891	6.7769	0.2237
892	7.0986	0.2288
893	7.4323	0.3094
894	7.7509	0.3660
895	8.1213	0.4262
896	8.5721	0.5109
897	9.1278	0.6320
898	9.8174	0.7933
899	10.6360	0.9676
901	11.5802	1.1792
902	12.6872	1.5589
903	14.0378	2.0738
905	14.5514	2.2847
906	15.9493	2.8979
907	17.6101	3.7321
908	19.5887	4.8460
909	21.7785	6.2456
910	24.1671	7.9669
911	26.6988	9.9795
913	29.3487	12.2908
914	32.2585	15.0579
915	35.5043	18.3890
916	39.0331	22.1330
917	42.8285	26.2791
918	46.9228	30.8892
927	47.7921	31.8583
928	52.9093	37.6225
929	58.4066	43.6930
930	64.8185	50.5630
931	72.1736	57.8177
932	80.1665	65.2855
935	84.5073	69.1958
933	88.7551	72.7243
936	92.3206	75.5388
937	101.0256	81.8635
864	106.4452	85.6115
938	108.0245	86.6437
865	117.4987	92.7289

Table 8. (Continued)

Block no.	$T_{ave}$ ( $^{\circ}$ K)	$Q/\Delta T$
866	127.7983	98.8153
867	144.2778	107.4603
868	168.3120	118.3373
869	193.7499	128.1180
871	218.7760	136.4295
872	242.4004	143.5927
845	245.7767	144.6157
839	252.4420	146.6236
846	259.2860	148.3826
840	261.6958	149.1316
874	263.2380	149.4621
875	266.5193	150.2409
847	268.7354	150.9203
876	269.3291	151.1167
841	270.7786	151.2143
877	271.3411	151.5307
852	272.4360	151.6273
878	273.2427	151.9238
879	274.8919	151.8656
853	275.5178	152.4992
940	275.7471	152.9627
854	276.9126	152.6414
941	277.1211	153.3604
855	278/0913	153.3348
942	278.3997	153.9353
856	279.2668	154.0024
943	279.4036	155.0230
842	279.6594	155.4815
849	279.6970	157.3896
944	280.2810	155.1396
857	280.4316	155.5006
945	281.0371	156.1271
858	281.5701	160.4899
946	281.7332	161.0553
947	282.3662	162.5796
859	282.6992	158.9461
948	283.0100	155.4485
949	283.6680	155.6250
860	283.8486	155.7601
950	284.4556	155.1406
880	284.5935	155.4063
861	285.0056	157.4097
951	285.8401	154.9535

Table 8. (Continued)

Block no.	$T_{\text{ave}}(^{\circ}\text{K})$	$Q/\Delta T$
862	287.2227	154.6843
952	288.3303	156.1404
843	288.4087	155.7385
850	288.8579	156.2715
953	292.5088	157.0636
881	294.3296	157.5647
882	296.0745	157.6556
883	298.7080	157.9299

Table 9. Lattice contribution to the thermodynamic functions of  $\text{CdCl}_2 \cdot 6\text{H}_2\text{O}$  for  $T \leq 14^{\circ}\text{K}$  (joules mole<sup>-1</sup> deg.<sup>-1</sup> mole wt. = 371.69 gm.)

$T(^{\circ}\text{K})$	$C_{\text{LATTICE}}$	$S_T^{\circ}$	$(H_T^{\circ} - H_0^{\circ})/T$	$-(F_T^{\circ} - H_0^{\circ})/T$
1.000	0.001	0.000	0.000	0.000
2.000	0.012	0.004	0.003	0.001
3.000	0.040	0.013	0.010	0.003
4.000	0.096	0.032	0.024	0.008
5.000	0.210	0.065	0.049	0.016
6.000	0.410	0.120	0.092	0.028
7.000	0.600	0.201	0.154	0.047
8.000	1.100	0.317	0.244	0.073
9.000	1.620	0.475	0.367	0.108
10.000	2.255	0.678	0.523	0.155
11.000	2.990	0.927	0.713	0.213
12.000	3.835	1.222	0.937	0.285
13.000	4.795	1.566	1.196	0.370
14.000	5.860	1.959	1.490	0.469

Table 10. Lattice plus magnetic contributions to the thermodynamic functions of  $\text{GdCl}_3 \cdot 6\text{H}_2\text{O}$  (joules mole<sup>-1</sup>deg.<sup>-1</sup>, mole wt. = 371.69 gm.)

$T(^{\circ}\text{K})$	$C_p$	$S_T^0$	$(H_T^0 - H_0^0)/T$	$-(F_T^0 - H_0^0)/T$
0.040	0.007	0.001	0.001	0.000
0.080	0.748	0.144	0.123	0.021
0.120	2.532	0.776	0.621	0.154
0.160	4.122	1.733	1.308	0.426
0.200	5.206	2.779	1.987	0.791
0.240	5.843	3.790	2.582	1.208
0.280	6.134	4.717	3.073	1.644
0.320	6.170	5.541	3.460	2.081
0.360	6.031	6.261	3.754	2.506
0.400	5.780	6.884	3.970	2.914
0.440	5.466	7.420	4.121	3.299
0.480	5.124	7.881	4.219	3.663
0.520	4.775	8.278	4.275	4.003
0.560	4.434	8.619	4.298	4.321
0.600	4.110	8.914	4.297	4.617
0.600	4.110	8.914	4.297	4.617
0.800	2.812	9.905	4.076	5.829
1.000	1.986	10.437	3.734	6.703
1.400	1.100	10.946	3.092	7.854
1.800	0.720	11.172	2.603	8.569
2.200	0.480	11.290	2.236	9.054
2.600	0.360	11.361	1.957	9.404
3.000	0.290	11.407	1.739	9.668
3.400	0.250	11.441	1.566	9.875
3.800	0.240	11.468	1.427	10.041
4.200	0.240	11.492	1.314	10.178
4.600	0.260	11.514	1.221	10.293
5.000	0.300	11.538	1.146	10.392
6.000	0.470	11.607	1.018	10.588
7.000	0.740	11.699	0.959	10.740
8.000	1.140	11.823	0.956	10.867
9.000	1.660	11.986	1.004	10.982
10.000	2.280	12.191	1.099	11.092
11.000	3.010	12.443	1.239	11.203
12.000	3.840	12.739	1.420	11.319
13.000	4.800	13.084	1.643	11.441
14.000	5.860	13.477	1.905	11.572
15.000	7.050	13.922	2.208	11.714
16.000	8.310	14.416	2.550	11.867
17.000	9.640	14.960	2.928	12.033
18.000	11.040	15.551	3.340	12.211
19.000	12.520	16.188	3.784	12.404
20.000	14.040	16.868	4.258	12.610

Table 10. (Continued)

T(°K)	$c_p$	$s_T^0$	$(H_T^0 - H_0^0)/T$	$-(F_T^0 - H_0^0)/T$
22.000	17.220	18.354	5.291	13.063
24.000	20.640	19.998	6.427	13.572
26.000	24.190	21.789	7.655	14.134
28.000	27.890	23.716	8.967	14.749
30.000	31.690	25.769	10.355	15.414
32.000	35.580	27.938	11.809	16.129
34.000	39.600	30.216	13.326	16.890
36.000	43.630	32.593	14.897	17.696
38.000	47.670	35.060	16.515	18.544
40.000	51.700	37.607	18.174	19.433
45.000	61.770	44.278	22.459	21.820
50.000	71.770	51.305	26.891	24.414
55.000	81.620	58.611	31.422	27.189
60.000	91.180	66.125	36.006	30.119
65.000	100.320	73.787	40.604	33.183
70.000	109.130	81.544	45.184	36.360
75.000	117.750	89.368	49.736	39.633
80.000	126.140	97.236	54.249	42.987
90.000	141.960	113.024	63.132	49.892
100.000	156.640	128.748	71.756	56.992
110.000	170.660	144.340	80.115	64.225
120.000	184.100	159.768	88.222	71.545
130.000	196.970	175.016	96.097	78.919
140.000	209.240	190.064	103.742	86.322
150.000	221.040	204.906	111.172	93.734
160.000	232.480	219.539	118.398	101.141
170.000	243.510	233.966	125.435	108.531
180.000	253.970	248.184	132.289	115.895
190.000	263.940	262.184	138.957	123.227
200.000	273.510	275.967	145.446	130.520
210.000	282.870	289.538	151.768	137.770
220.000	291.830	302.906	157.932	144.973
230.000	300.480	316.071	163.944	152.127
240.000	308.760	329.035	169.807	159.228
250.000	316.820	341.802	175.526	166.277
260.000	324.630	354.380	181.110	173.270
270.000	332.410	366.778	186.570	180.208
273.150	334.870	370.640	188.270	182.350
280.000	340.200	379.008	191.918	187.090
290.000	347.900	391.080	197.164	193.916
298.150	354.130	400.800	201.370	199.430
300.000	355.520	403.003	202.316	200.687

Table 11. Thermodynamic functions of  $\text{TbCl}_3 \cdot 6\text{H}_2\text{O}$  (joules mole<sup>-1</sup>deg.<sup>-1</sup>, mole wt. = 373.36 gm.)

$T(^{\circ}\text{K})$	$c_p$	$S_T^{\circ}$	$(H_T^{\circ}-H_0^{\circ})/T$	$-(F_T^{\circ}-H_0^{\circ})/T$
1.000	0.200	0.140	0.087	0.053
2.000	0.500	0.348	0.202	0.147
3.000	1.400	0.633	0.378	0.255
4.000	2.180	1.171	0.756	0.415
5.000	2.350	1.680	1.061	0.619
6.000	2.320	2.111	1.278	0.833
7.000	2.400	2.471	1.430	1.041
8.000	2.640	2.806	1.565	1.241
9.000	3.040	3.139	1.706	1.434
10.000	3.570	3.486	1.864	1.621
11.000	4.250	3.857	2.049	1.807
12.000	5.070	4.260	2.266	1.995
13.000	6.130	4.707	2.521	2.186
14.000	7.360	5.206	2.822	2.383
15.000	8.700	5.759	3.169	2.590
16.000	10.120	6.365	3.559	2.806
17.000	11.600	7.023	3.988	3.035
18.000	13.170	7.730	4.454	3.276
19.000	14.810	8.486	4.956	3.530
20.000	16.490	9.288	5.490	3.798
22.000	20.030	11.025	6.651	4.374
24.000	23.760	12.927	7.921	5.007
26.000	27.530	14.978	9.284	5.694
28.000	31.450	17.160	10.725	6.434
30.000	35.500	19.465	12.239	7.226
32.000	39.570	21.885	13.819	8.066
34.000	34.660	24.318	15.366	8.952
36.000	47.730	26.841	16.968	9.873
38.000	51.860	29.533	18.696	10.837
40.000	56.000	32.298	20.458	11.840
45.000	66.290	39.489	24.979	14.509
50.000	76.580	47.004	29.624	17.381
55.000	86.650	54.782	34.357	20.426
60.000	96.060	62.728	39.109	23.619
65.000	105.280	70.782	43.846	26.936
70.000	114.180	78.912	48.554	30.358
75.000	122.790	87.084	53.216	33.867
80.000	131.360	95.283	57.833	37.450
90.000	147.470	111.703	66.915	44.788
100.000	162.050	128.005	75.709	52.296
110.000	175.810	144.101	84.189	59.912
120.000	189.080	159.971	92.380	67.591
130.000	201.780	175.611	100.311	75.300



Table 11. (Continued)

$T(^{\circ}\text{K})$	$C_p$	$S_T^{\circ}$	$(H_T^{\circ}-H_0^{\circ})/T$	$-(F_T^{\circ}-H_0^{\circ})/T$
140.000	213.900	191.012	107.995	83.016
150.000	225.510	206.169	115.447	90.723
160.000	236.630	221.081	122.675	98.405
170.000	247.280	235.747	129.693	106.054
180.000	257.530	250.173	136.512	113.661
190.000	267.380	264.363	143.142	121.220
200.000	276.620	278.315	149.588	128.727
210.000	285.410	292.026	155.848	136.178
220.000	293.900	305.500	161.931	143.569
230.000	302.180	318.747	167.849	150.898
240.000	310.320	331.780	173.616	158.164
250.000	318.340	344.611	179.245	165.366
260.000	326.210	357.250	184.747	172.503
270.000	333.850	369.706	190.129	179.577
273.157	336.230	373.570	191.790	181.740
280.000	341.320	381.982	195.396	186.587
290.000	348.650	394.087	200.554	193.534
298.150	354.490	403.840	204.690	199.150
300.000	355.760	406.027	205.609	200.418

Table 12. Thermodynamic functions of  $\text{HoCl}_3 \cdot 6\text{H}_2\text{O}$  (joules mole<sup>-1</sup>deg.<sup>-1</sup>, mole wt. = 379.37 gm.)

$T(^{\circ}\text{K})$	$C_p$	$S_T^{\circ}$	$(H_T^{\circ}-H_0^{\circ})/T$	$-(F_T^{\circ}-H_0^{\circ})/T$
1.000	0.120	0.087	0.053	0.033
2.000	0.540	0.258	0.162	0.097
3.000	2.290	0.785	0.561	0.225
4.000	3.950	1.696	1.222	0.474
5.000	4.800	2.674	1.857	0.817
6.000	5.480	3.612	2.407	1.205
7.000	6.100	4.504	2.891	1.613
8.000	6.670	5.356	3.328	2.028
9.000	7.220	6.174	3.730	2.444
10.000	7.770	6.963	4.106	2.856
11.000	8.330	7.730	4.465	3.265
12.000	8.930	8.480	4.812	3.668
13.000	9.680	9.223	5.156	4.067
14.000	10.570	9.972	5.511	4.462

Table 12. (Continued)

$T(^{\circ}\text{K})$	$C_p$	$S_T^{\circ}$	$(H_T^{\circ}-H_0^{\circ})/T$	$-(F_T^{\circ}-H_0^{\circ})/T$
15.000	11.560	10.735	5.881	4.854
16.000	12.650	11.516	6.269	5.246
17.000	13.840	12.318	6.679	5.639
18.000	15.100	13.144	7.112	6.032
19.000	16.430	13.996	7.567	6.429
20.000	17.840	14.874	8.044	6.829
22.000	20.840	16.712	9.069	7.643
24.000	24.090	18.663	10.184	8.480
26.000	27.500	20.725	11.384	9.342
28.000	31.070	22.893	12.661	10.231
30.000	34.770	25.162	14.011	11.151
32.000	38.590	27.527	15.427	12.100
34.000	42.510	29.984	16.905	13.079
36.000	46.480	32.526	18.437	14.088
38.000	50.450	35.145	20.018	15.127
40.000	54.420	37.834	21.639	16.195
45.000	64.400	44.819	25.835	18.984
50.000	74.320	52.119	30.189	21.931
55.000	84.070	59.661	34.645	25.016
60.000	93.600	67.386	39.162	28.224
65.000	102.780	75.245	43.707	31.538
70.000	111.540	83.182	48.239	34.943
75.000	120.100	91.171	52.746	38.425
80.000	128.470	99.190	57.218	41.972
90.000	144.220	115.246	66.024	49.222
100.000	158.820	131.208	74.584	56.624
110.000	172.460	146.987	82.864	64.123
120.000	185.780	162.568	90.889	71.679
130.000	198.470	177.945	98.681	79.263
140.000	210.640	193.100	106.246	86.854
150.000	222.300	208.034	113.598	94.437
160.000	233.340	222.737	120.740	101.997
170.000	243.870	237.201	127.675	109.526
180.000	254.010	251.428	134.413	117.015
190.000	263.840	265.426	140.967	124.459
200.000	273.280	279.200	147.348	131.852
210.000	282.230	292.752	153.559	139.192
220.000	290.800	306.079	159.603	146.476
230.000	299.210	319.191	165.490	153.701
240.000	307.410	332.099	171.234	160.866
250.000	315.390	344.811	176.841	167.970
260.000	323.070	357.331	182.318	175.012
270.000	330.620	369.665	187.671	181.994

Table 12. (Continued)

$T(^{\circ}\text{K})$	$C_p$	$S_T^{\circ}$	$(H_T^{\circ}-H_0^{\circ})/T$	$-(F_T^{\circ}-H_0^{\circ})/T$
273.150	332.970	373.490	189.320	184.150
280.000	338.080	381.823	192.909	188.914
290.000	345.500	393.816	198.043	195.773
298.150	351.600	403.510	202.140	201.300
300.000	353.000	405.655	203.083	202.572

Table 13. Thermodynamic functions of  $\text{LuCl}_3 \cdot 6\text{H}_2\text{O}$  (joules mole<sup>-1</sup>deg.<sup>-1</sup>, mole wt. = 389.41 gm.)

$T(^{\circ}\text{K})$	$C_p$	$S_T^{\circ}$	$(H_T^{\circ}-H_0^{\circ})/T$	$-(F_T^{\circ}-H_0^{\circ})/T$
1.000	0.001	0.000	0.000	0.000
2.000	0.012	0.004	0.003	0.001
3.000	0.030	0.013	0.010	0.003
4.000	0.068	0.026	0.018	0.007
5.000	0.155	0.048	0.035	0.013
6.000	0.340	0.092	0.069	0.022
7.000	0.625	0.164	0.127	0.037
8.000	1.040	0.273	0.214	0.059
9.000	1.550	0.424	0.334	0.091
10.000	2.140	0.618	0.484	0.134
11.000	2.820	0.853	0.665	0.188
12.000	3.600	1.131	0.876	0.255
13.000	4.480	1.453	1.119	0.334
14.000	5.460	1.820	1.394	0.427
15.000	6.530	2.233	1.700	0.533
16.000	7.680	2.691	2.038	0.654
17.000	8.920	3.194	2.405	0.788
18.000	10.220	3.741	2.804	0.937
19.000	11.570	4.329	3.229	1.100
20.000	12.980	4.958	3.681	1.277
22.000	15.950	6.333	4.660	1.673
24.000	19.120	7.855	5.732	2.123
26.000	22.390	9.515	6.887	2.627
28.000	25.770	11.298	8.115	3.182
30.000	29.270	13.193	9.407	3.786
32.000	32.910	15.198	10.762	4.436
34.000	36.640	17.305	12.174	5.130

Table 13. (Continued)

$T(^{\circ}\text{K})$	$C_p$	$S_T^{\circ}$	$(H_T^{\circ}-H_0^{\circ})/T$	$-(F_T^{\circ}-H_0^{\circ})/T$
36.000	40.390	19.505	13.638	5.868
38.000	44.170	21.790	15.145	6.645
40.000	47.910	24.151	16.690	7.461
45.000	57.320	30.336	20.680	9.656
50.000	66.810	36.864	24.816	12.047
55.000	76.110	43.670	29.059	14.611
60.000	85.200	50.684	33.360	17.324
65.000	94.130	57.859	37.694	20.165
70.000	102.750	65.151	42.034	23.117
75.000	111.200	72.529	46.364	26.165
80.000	119.420	79.970	50.675	29.295
90.000	135.160	94.954	59.197	35.757
100.000	149.740	109.956	67.529	42.427
110.000	163.620	124.882	75.637	49.245
120.000	177.150	139.702	83.535	56.167
130.000	190.030	154.397	91.238	63.159
140.000	202.220	168.930	98.734	70.196
150.000	213.910	183.282	106.025	77.257
160.000	225.290	197.453	113.125	84.328
170.000	236.250	211.441	120.047	91.395
180.000	246.800	225.245	126.796	98.448
190.000	256.890	238.862	133.382	105.481
200.000	266.420	252.283	139.797	112.486
210.000	275.550	265.504	146.045	119.459
220.000	284.500	278.530	152.136	126.394
230.000	293.230	291.369	158.081	133.288
240.000	301.820	304.031	163.892	140.139
250.000	310.120	316.521	169.576	146.945
260.000	318.110	328.840	175.136	153.704
270.000	325.610	340.990	180.574	160.416
272.000	326.900	343.398	181.645	161.753
273.150	327.610	344.770	182.250	162.510
274.000	328.250	345.798	182.710	163.087
276.000	330.000	348.191	183.771	164.420
277.000	331.190	349.386	184.301	165.085
278.000	332.700	350.582	184.832	165.750
279.000	334.870	351.780	185.365	166.415
280.000	338.600	352.984	185.905	167.079
280.500	341.700	353.591	186.180	167.411
281.000	345.800	354.202	186.460	167.742
281.500	352.000	354.822	186.748	168.074
282.000	378.800	355.464	187.058	168.406
282.500	359.400	356.117	187.380	168.737
283.000	346.350	256.740	187.671	169.069

Table 13. (Continued)

T(°K)	C <sub>p</sub>	S <sub>T</sub> <sup>0</sup>	(H <sub>T</sub> <sup>0</sup> -H <sub>0</sub> <sup>0</sup> )/T	-(F <sub>T</sub> <sup>0</sup> -H <sub>0</sub> <sup>0</sup> )/T
283.500	338.700	357.344	187.943	169.400
284.000	337.250	357.939	188.207	169.732
284.500	336.750	358.531	188.469	170.063
285.000	336.650	359.122	188.729	170.394
285.500	336.850	359.712	188.988	170.725
286.000	337.250	360.302	189.247	171.055
288.000	339.910	362.661	190.284	172.378
290.000	342.020	365.021	191.323	173.698
292.000	343.450	367.377	192.361	175.016
294.000	344.370	369.725	193.392	176.333
296.000	344.950	372.061	194.414	177.647
298.000	345.300	374.385	195.426	178.960
298.150	345.320	374.540	195.520	179.060
300.000	345.500	376.696	196.426	180.270

In the case of Tb<sup>+3</sup> this number would be 13 from the <sup>7</sup>F<sub>6</sub> state and in the case of Ho<sup>+3</sup>, 17 from <sup>5</sup>I<sub>8</sub>.

As discussed in the introduction, the thermal population of crystal field levels leads to a contribution to the heat capacities of these salts. The heat capacities of the Gd and Lu salts were measured in order that the lattice contributions to the heat capacities of the magnetic salts could be estimated. The magnetic contributions to the heat capacities of the Tb and Ho salts were obtained by subtracting the lattice contributions from the original data points, according to equation 11 (Gerstein, 1960).

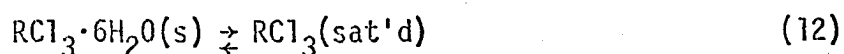
$$C_M = \frac{1}{\alpha} [Q/\Delta T(R+\text{add.}) - \frac{\alpha}{\beta} Q/\Delta T(Lu+\text{add.}) + (\frac{\alpha-\beta}{\beta}) Q/\Delta T(\text{add.})] - \alpha C_{\text{lattice}} \quad (11)$$

Here, the Lu data were taken to provide the lattice contribution and the last term served to correct for the variation of this contribution across

the series. The symbols  $\alpha$  and  $\beta$  represent the numbers of moles of the magnetic salt and of the Lu salt respectively. The importance of maintaining  $\alpha/\beta$  is seen in the third term, in that the heat capacity of the addenda tends to cancel from the calculations.  $\Delta C_{\text{lattice}}$  was determined for each of the magnetic salts by a linear interpolation between the Gd and Lu data. Implicit in this procedure is the assumption that  $(C_p - C_v)$  is constant between these two salts. Figures 11 and 12 show the magnetic heat capacities of the Tb and Ho salts.

### C. Solution Entropies

Equation 12 describes the process: the crystalline solid at the temperature and pressure in question, in equilibrium with the solute in the saturated solution.



Here the solute in solution is considered to be the hydrated species. For this equilibrium, the free energy change is zero. The entropy change can then be calculated from the enthalpy change, which is given by:

$$\Delta H = \bar{H}_2(\text{sat'd}) - \bar{H}_2^{\cdot} \quad (13)$$

Here the superscript ( $\cdot$ ) denotes the pure solid component 2, i.e., the solute. This equation can be rewritten as:

$$\Delta H = \bar{H}_2(\text{sat'd}) - \bar{H}_2^{\circ} - \bar{H}_2^{\cdot} + \bar{H}_2^{\circ} \quad (14)$$

or,

$$\Delta H = \bar{L}_2(\text{sat'd}) - \bar{L}_2^{\cdot} \quad (15)$$

Figure 11. Magnetic heat capacity of  $\text{TbCl}_3 \cdot 6\text{H}_2\text{O}$

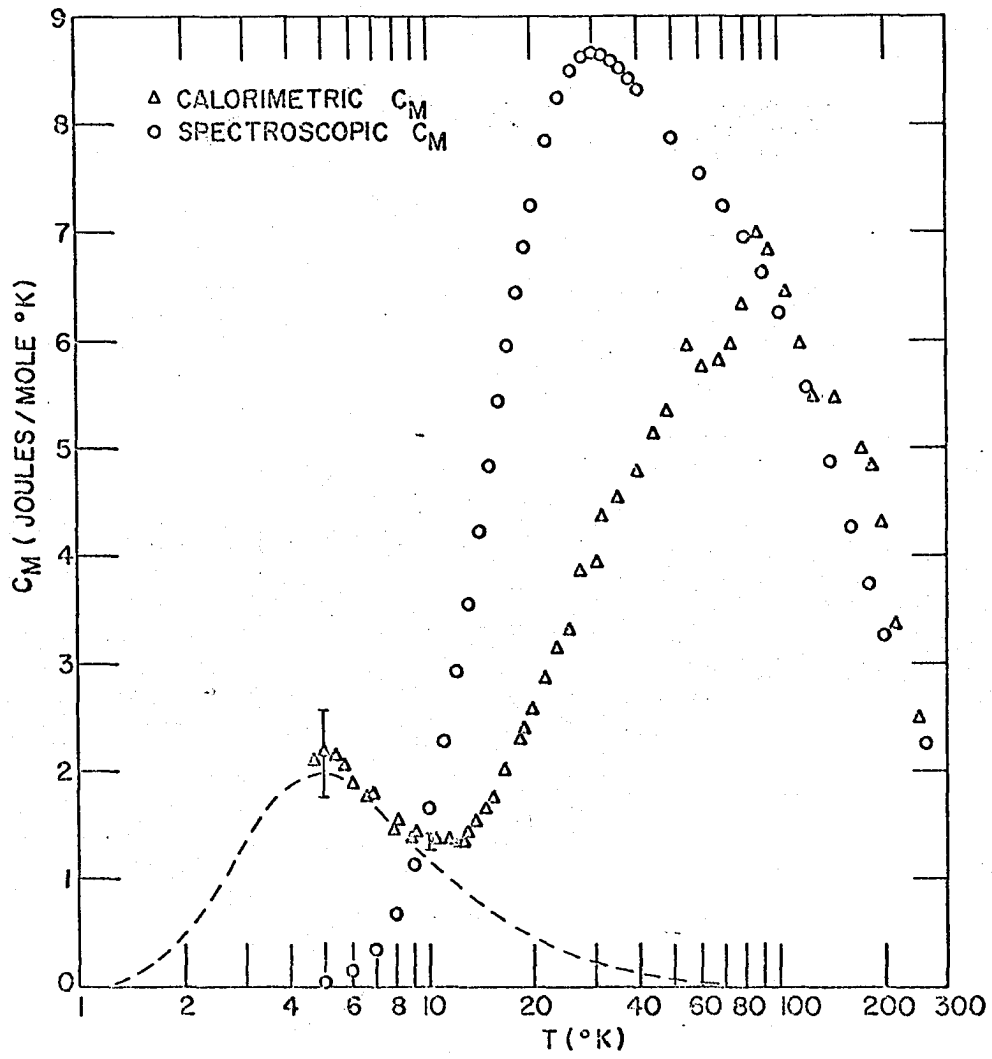
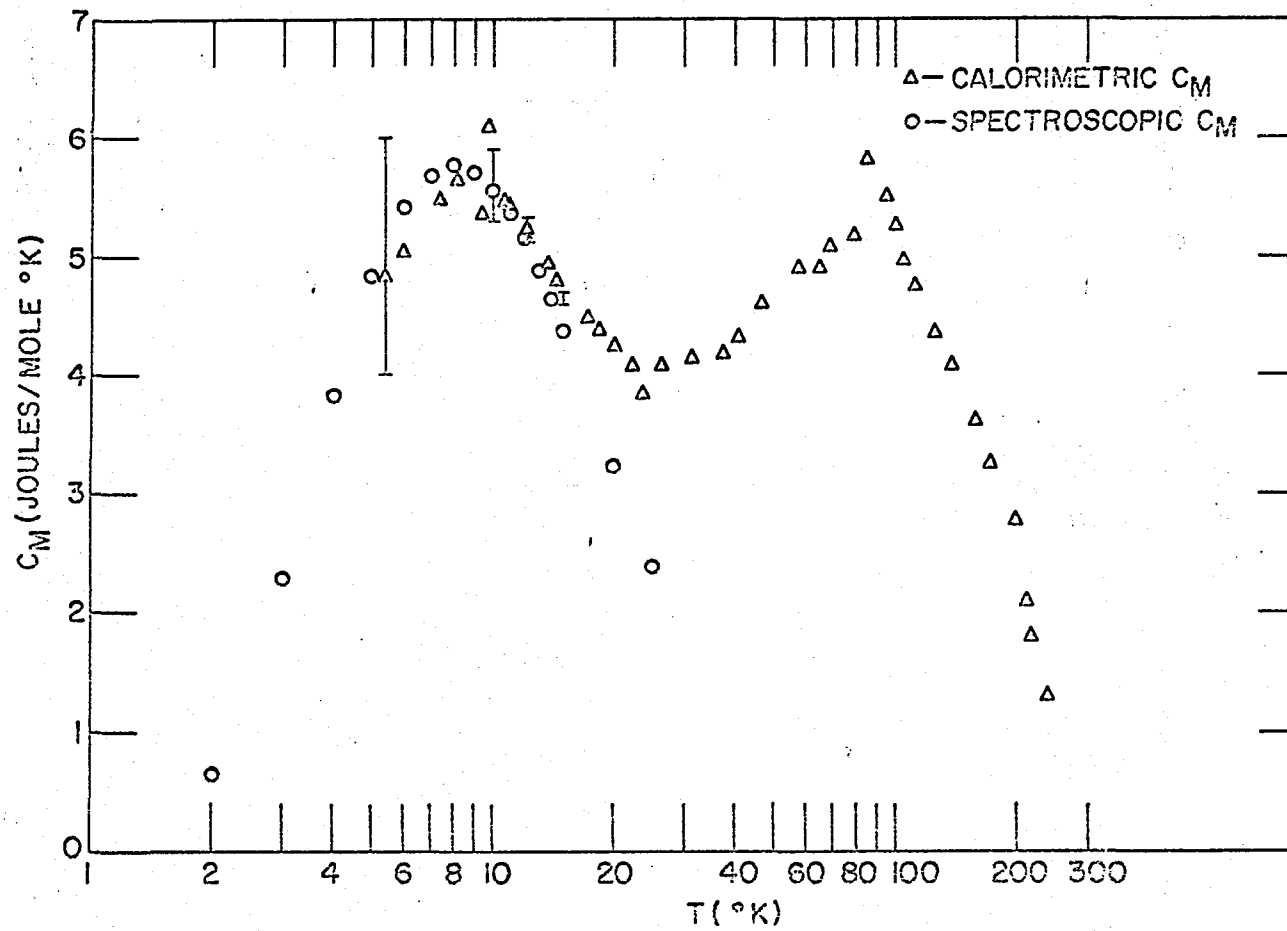




Figure 12. Magnetic heat capacity of  $\text{HoCl}_3 \cdot 6\text{H}_2\text{O}$



Both terms on the right hand side of equation 15 are available from solution calorimetry (Pepple, 1967; DeKock, 1965). Similarly the entropy change is given by:

$$\Delta S = \bar{S}_2(\text{sat'd}) - \bar{S}_2^{\cdot} \quad (16)$$

or,

$$\Delta S = [\bar{S}_2(\text{sat'd}) - \bar{S}_2^{\times}] - S_2^{\cdot} + \bar{S}_2^{\times} \quad (17)$$

Here  $\bar{S}_2^{\cdot} \equiv S_T^0$ , the absolute entropy of the crystal, as determined from the present measurements, and  $[\bar{S}_2(\text{sat'd}) - \bar{S}_2^{\times}]$  is the partial molal excess entropy as determined from solution calorimetry (Pepple, 1967; DeKock, 1965). Then, since

$$\Delta H = T\Delta S \quad (18)$$

it follows from equations 15 and 17 that

$$\bar{S}_2^{\times} = T^{-1}[\bar{L}_2(\text{sat'd}) - \bar{L}_2^{\cdot}] - [\bar{S}_2(\text{sat'd}) - \bar{S}_2^{\cdot}] + S_T^0 \quad (19)$$

The values of  $\bar{S}_2^{\times}$  for the salts studied here are listed in Table 14. In principle, the partial molal entropy of the rare earth ion can be obtained by subtracting the contributions to the solute partial molal entropy from the chloride ions and the water molecules in the hydration sphere. This process involves arbitrarily choosing the values of the chloride ion contributions and the result is thus in no sense an "absolute" entropy. The first two columns in Table 14 list the salts for which the entropies have been determined in this present work, and those entropies at 298.15<sup>0</sup>K, respectively. The next three columns list the solution calorimetry results

obtained by DeKock (1965) and by Pepple (1967). The last column gives the entropies from equation 19. The approach used here to obtain  $\bar{S}_2^0$  will be discussed further in another section.

Table 14. Standard state entropies (calories mole<sup>-1</sup> deg<sup>-1</sup>, T = 298.15°K)

Salt	$S_f^0$	$\bar{L}_2(\text{sat'd})$	$\bar{L}_2^*$	$T[\bar{S}_2(\text{sat'd}) - \bar{S}_2^*]$	$\bar{S}_2^*$
GdCl <sub>3</sub> ·6H <sub>2</sub> O	97.17	15,577	9,112	11,402	80.61 <sup>a</sup>
TbCl <sub>3</sub> ·6H <sub>2</sub> O	96.52	16,260	9,556	11,870	79.19
HoCl <sub>3</sub> ·6H <sub>2</sub> O	96.44	16,720	10,426	11,590	78.68
LuCl <sub>3</sub> ·6H <sub>2</sub> O	89.52	17,736	11,851	10,944	72.55

$$^a \bar{S}_2^* = \bar{S}_2^0 - \nu R \ln m_f$$

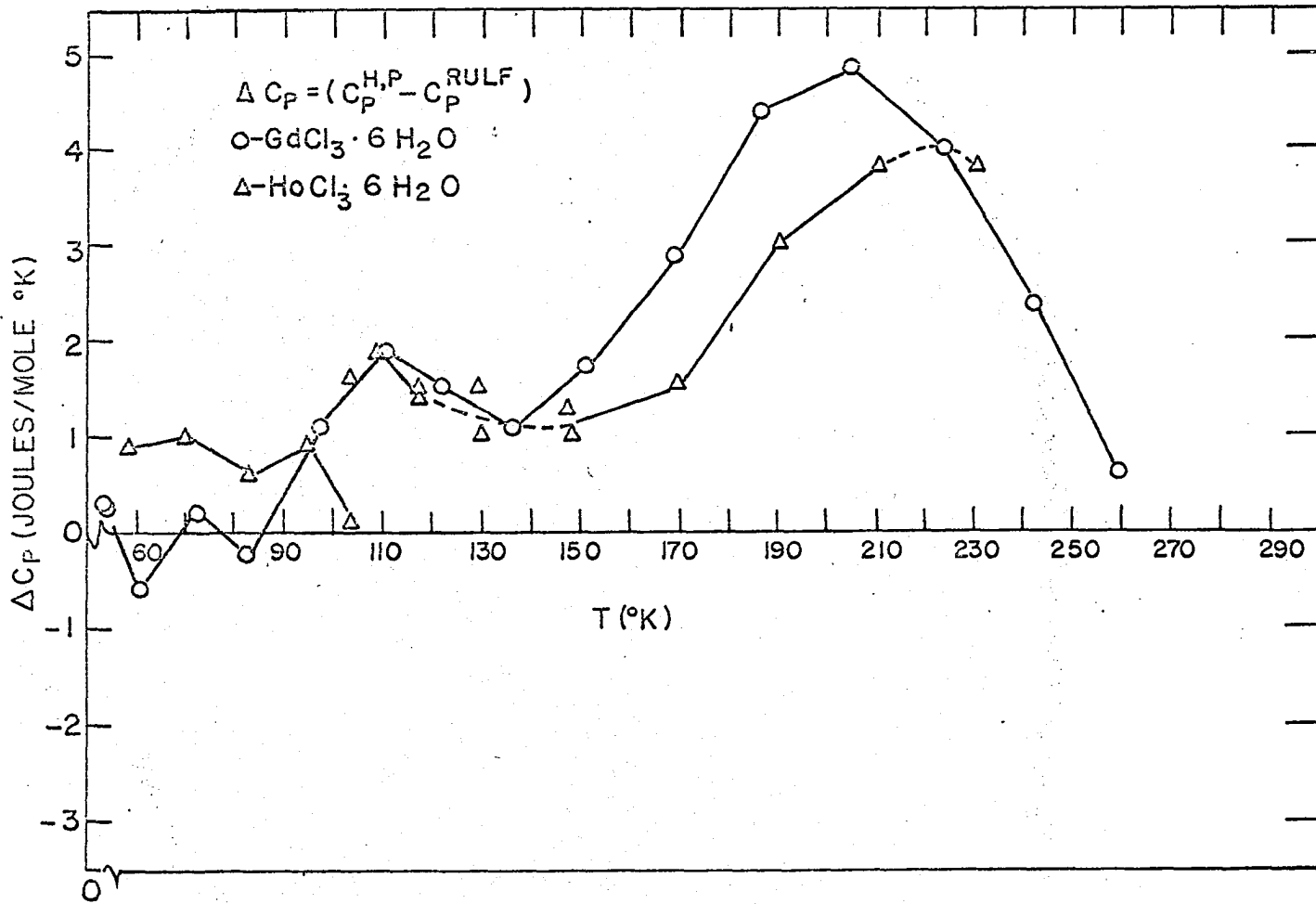
## V. DISCUSSION

## A. Heat Capacities

Previously published heat capacity measurements on several of the salts studied here have already been mentioned. In particular, Hellwege et al. (1961) and Pfeffer (1961a, 1962) have made measurements on the Gd and on the Ho and Lu salts respectively. Figure 13 relates the present and previous results for the Gd and Ho salts. The bumps above  $100^{\circ}\text{K}$  were caused by the presence of occluded water in the crystals used by the latter authors (see the discussion under "Sample"). The maximum magnitudes of these "water bumps" is of the order of 2% of the heat capacity e.g., in the case of the Gd salt. Below  $100^{\circ}\text{K}$ , the heat capacity results tend to be insensitive to the presence of occluded water. The irregularity in the range  $110^{\circ}\text{K} \leq T \leq 150^{\circ}\text{K}$  is difficult to explain on the basis of the available information. However, the discontinuity in Pfeffer's values at  $104^{\circ}\text{K}$  suggests the possibility of a discontinuity in his thermometer table. The difference function in the case of the Lu salt is similar to the curves shown. The behavior of the Lu curve is not nearly as striking however, because the water bump becomes obvious only above  $200^{\circ}\text{K}$ , near the highest temperatures reported. The heat capacity of the Tb salt has not been previously reported.

The anomalous behavior of the heat capacity of the Lu salt has been briefly discussed in an earlier section. It was shown there that occluded water was most likely not the cause of the bump. Another possible explanation was the occurrence of a structural change in the crystal at about  $280^{\circ}\text{K}$ . Considerable evidence exists that all of the salts studied here are

Figure 13. Difference function relating the present and some previously published  $\text{GdCl}_3 \cdot 6\text{H}_2\text{O}$  and  $\text{HoCl}_3 \cdot 6\text{H}_2\text{O}$  heat capacities

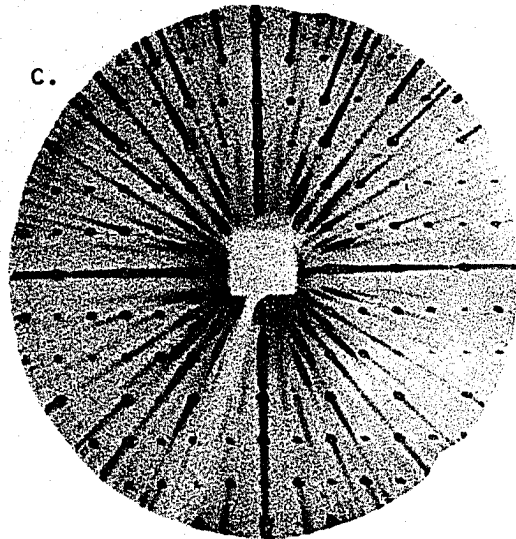
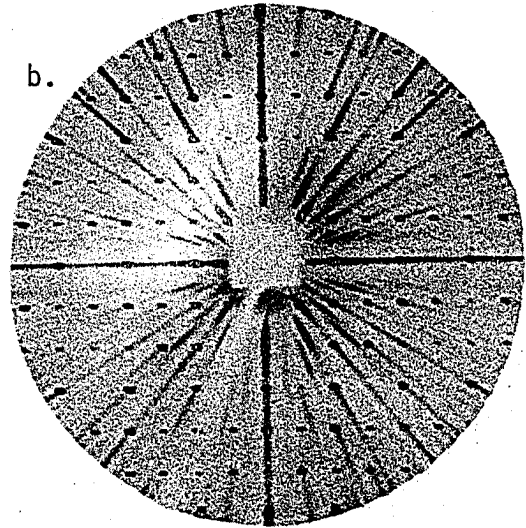
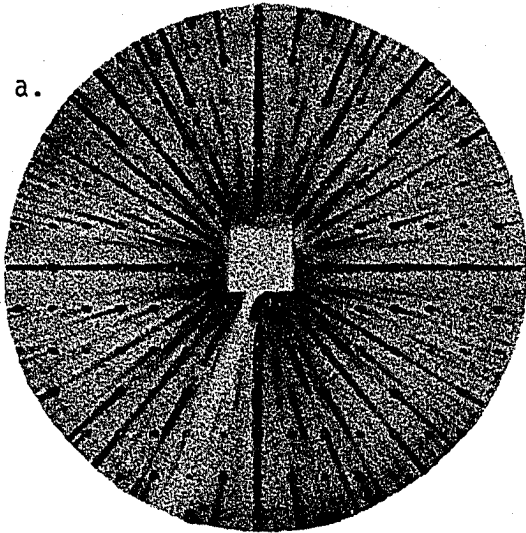


isostructural. Thus Marezio, et al. (1961) and Bel'skii and Struchkov (1965) have determined the structures of the Gd and Eu salts respectively, and have found them to be completely analogous. Graeber, et al. (1966) have published the lattice constants of the salts of the members of the series from Sm through Tm. The latter authors found that, in accordance with the lanthanide contraction, the unit cell volumes decrease approximately linearly across the series.

In order to investigate the possibility of a structure change in the Lu salt, two sets of x-ray photographs were obtained. The first set consisted of powder photographs of the Ho and the Lu salts. Comparison of the films indicated that these two salts are isostructural at room temperature. The second set consisted of two precession photographs of a single crystal of  $\text{LuCl}_3 \cdot 6\text{H}_2\text{O}$  at two different temperatures. Figure 14 shows these photographs. The sample was at room temperature for the exposure in part (a), and at about 220°K in part (b). Part (c) shows the two photographs superimposed. To the extent that the spots represent dimensionless points, the photographs give a mapping of the reciprocal lattice. Each point in the reciprocal lattice corresponds to a set of planes in the lattice of the crystal. Thus the comparison in part (c) indicates that the crystal is isostructural with respect to the size and shape of the unit cell on each side of the heat capacity anomaly. Further comparison of the photographs, for which the exposure times were not identical, suggests from the relative intensities that there is probably no minor shift in the positions of the heavier atoms that could be readily associated with the anomaly.



Figure 14. Precession photographs of a single crystal of  $\text{LuCl}_3 \cdot 6\text{H}_2\text{O}$



## B. Magnetic Heat Capacities

Evidence exists (Levy, 1964; Duffy et al., 1963; and Hellwege et al., 1961) that the ground state of  $Gd^{+3}$  in  $GdCl_3 \cdot 6H_2O$  is split by the crystal field to the extent of about 1 wave number. In order to obtain the lattice heat capacity of the Gd salt, it was necessary to account for the heat capacity contribution from this splitting.

The approach taken was to fit the low temperature ( $T \leq 3^0K$ ) data of Hellwege et al. (1961) with a heat capacity term based on a reasonable estimate of the energy level structure. The assumption was made that the  $^8S_{7/2}$  state splits into four equally spaced, doubly degenerate levels. The corresponding magnetic (or "Schottky") heat capacity was calculated from equation 20:

$$C_{Schottky} = \frac{\delta E}{\delta T} = \frac{Nk}{Z^2} \left[ Z \sum_{i=1}^n g_i \left( \frac{E_i}{kT} \right)^2 e^{-E_i/kT} - \left( \sum_{i=1}^n g_i \frac{E_i}{kT} e^{-E_i/kT} \right)^2 \right] \quad (20)$$

where

$$E = \frac{N \left( \sum_{i=1}^n g_i E_i e^{-E_i/kT} \right)}{\left( \sum_{i=1}^n g_i e^{-E_i/kT} \right)} \quad (21)$$

and

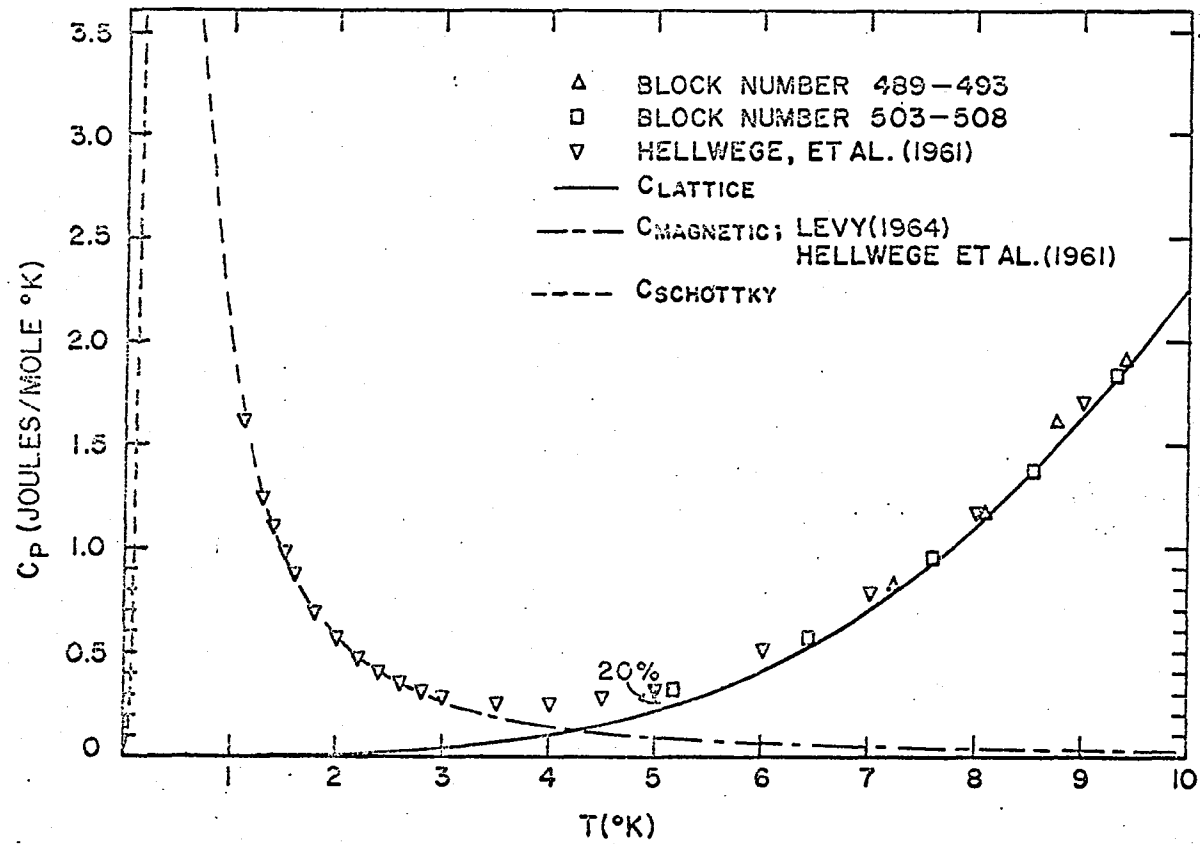
$$Z = \left( \sum_{i=1}^n g_i e^{-E_i/kT} \right) \quad (22)$$

$E$  is the average energy of the ensemble of representative systems.  $Z$  is the system partition function. The symbol  $n$  is the number of eigen states of each representative system. The symbols  $E_i$  and  $g_i$  are the energy relative to the ground level, and the degeneracy of level "i".

Figure 15 shows the heat capacity of  $\text{GdCl}_3 \cdot 6\text{H}_2\text{O}$  below  $10^\circ\text{K}$ . The Schottky heat capacity term and Hellwege's data agree to within several percent at temperatures for which the lattice term is relatively small. Moreover, the Schottky term also agrees well with the estimate of the magnetic contribution given by Levy (1964). This agreement suggests that the lattice term, obtained by subtracting the Schottky term from the measured heat capacity, is reliable to at least within the precision of my data below  $15^\circ\text{K}$ .

The magnetic contributions to the heat capacities of the Ho and Tb salts were compared with the optical spectroscopic results of Kahle (1956) and Dieke (1968). The energy levels published by these authors are shown in Figure 15. Figure 12 shows the magnetic heat capacity of  $\text{HoCl}_3 \cdot 6\text{H}_2\text{O}$  as a function of temperature, plotted for convenience on a logarithmic scale. The triangles represent the calorimetrically determined results. The error bars are associated with these points and represent the precision of the raw heat capacity data. Above about  $20^\circ\text{K}$ , the uncertainties involved in the subtraction of the lattice contribution become increasingly important and make it difficult to estimate the precision. It is reasonable though, to regard the high temperature points as being known to no better than  $\pm 8\%$ . The circles represent Kahle's (1956) results for the lowest four levels of the  $^5\text{I}_8$  term in  $\text{Ho}^{+3}$  in the trichloride hexahydrate, obtained from the absorption spectrum. The agreement is seen to be within experimental error. For the Tb results, there is a major difference between the calorimetric and the spectroscopic heat capacities as is shown in Figure 11. Again the triangles represent the calorimetric data. The heat capacity results require the existence of

Figure 15. Heat capacity of  $\text{GdCl}_3 \cdot 6\text{H}_2\text{O}$  in the temperature region below  $10^0\text{K}$

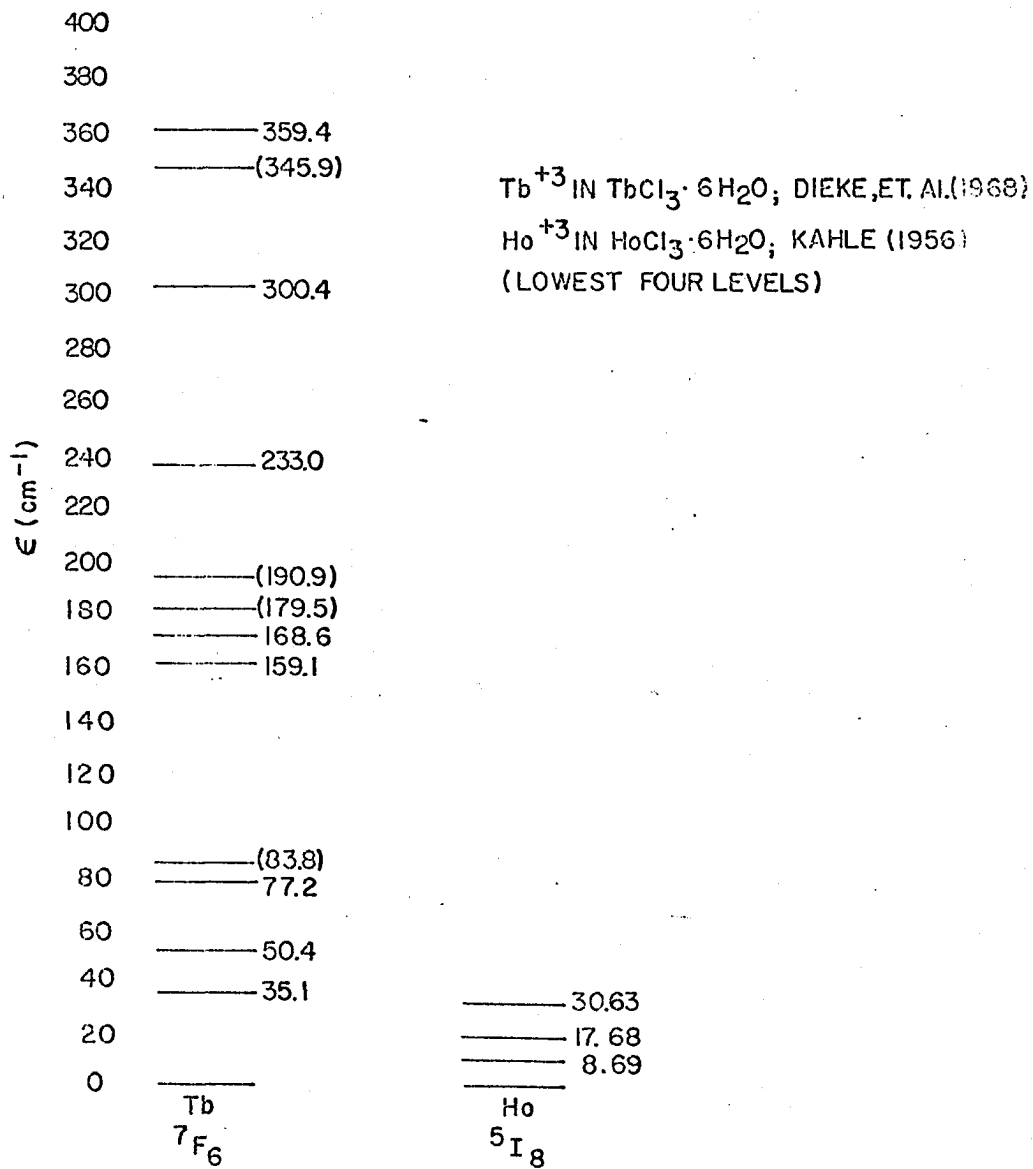


low-lying levels within approximately 8 wave numbers of the ground state. The results of Dieke (1968), from the fluorescence spectrum, have the lowest level at about 35 wave numbers. No estimate of the precision of these particular spectroscopic results has been given. However, the width of the lowest energy fluorescence band is such that quite possibly the spectrograph failed to resolve a relatively low intensity emission peak. The existence of such a low-lying level would require that a higher energy level had been improperly assigned. Figure 16 shows that there is some uncertainty indicated in, for example, the level at 83.8 wave numbers, as well as in several of the others.

The dashed curve in Figure 11 corresponds to a Schottky term (equation 19) involving two levels. The parameters  $g_1$  and  $E_1$  were chosen under the assumption that the lowest temperature heat capacity point represents a local maximum in the magnetic heat capacity. In the absence of heat capacity data below  $5^{\circ}\text{K}$  for the Tb salt, this approximation was used to extrapolate  $C_p$  to  $0^{\circ}\text{K}$  for the calculation of the thermodynamic functions. As the magnetic entropy is essentially fully developed at  $300^{\circ}\text{K}$ , the validity of this approach can be approximately checked. The magnitude of the entropy also serves as a check on the approximation to the lattice contribution. A comparison of the magnetic entropies of the Ho and Tb salts at  $300^{\circ}\text{K}$  shows that the values for the former salt is about 86% of  $R\ln(2J+1)$  while that for the latter is about 80% of  $R\ln(2J+1)$ . There is some justification for making such a comparison, in that the crystal field potentials for each case might reasonably be expected to be of the same order of magnitude. The comparison does suggest that if the magnetic entropy for the Tb salt is in error, it is probably low by several percent. In this

Figure 16. Ground state crystal field splittings from optical spectra





event, the error introduced in the total entropy  $S_T^0$  at room temperature is of the order of 0.25%. More certain conclusions must await the availability of heat capacity data for the Tb salt below 5°K.

### C. Solution Entropies

Extensive investigations of the thermodynamic and transport properties of aqueous rare earth salt solutions have been conducted in the Ames Laboratory over approximately the last twenty years. From these investigations it has been observed that many solution properties, such as  $\phi_V^0$ ,  $\phi_L$ , and  $\phi_{cp}$ , vary irregularly as functions of rare earth atomic number. The behavior of these properties is usually interpreted in terms of the expected interactions between the water molecules and the rare earth ions. It has been postulated that a rare earth ion, being strongly hydrated, and having a certain number of water molecules in its first hydration sphere, may exist in equilibrium with similar ions which have either a larger or smaller hydration sphere coordination number. As the ionic radius decreases with increasing atomic number, past a certain critical value, the equilibrium concentration shifts in favor of the species having the smaller coordination number. Thus, the radius of the first hydration sphere decreases with that of the rare earth ion until the mutually repulsive interactions among the water molecules cause the lower hydration number to represent the more favorable situation. The shift in the equilibrium is usually considered to take place gradually between Nd and Tb.

Among the properties which, for the rare earths, are non-linear in atomic number is  $(\bar{S}_2 - \bar{S}_2^M)$ , the partial molal excess entropy of the solute (DeKock, 1965; Pepple, 1967). On the basis of the above postulate, the

general decrease in  $(\bar{S}_2 - \bar{S}_2^{\text{cr}})$  with increase in atomic number has been interpreted as being the result of the ordering effect of the ions on the water molecules. The ions exhibit an increasing influence on the orientations of the surrounding water molecules as their charge densities increase. As the relative concentration of the lower hydrated species increases i.e., at a given total solute concentration,  $\bar{S}_2$  increases. This can be related to an expected increase in the freedom of motion of the solvent that results from there being a greater average number of water molecules outside the first hydration sphere.

There is a basic difficulty involved in making comparisons among the values of relative properties [such as  $(\bar{S}_2 - \bar{S}_2^{\text{cr}})$ ] of different chemical systems. It is that differences among the standard state values of thermodynamic properties may be significant in the comparison of relative properties. In the present case it might be desirable to compare the magnetic contributions to  $\bar{S}_2$  for say, the odd and even atomic numbered rare earths. In the case of relative partial molal entropies, the absolute values of the solutes are available from the third law entropy of the salt and the existing results of measurements of solution thermodynamic properties. When heat capacity results of the type presented here become available for more members of the series, it will be possible to make more meaningful comparisons among the partial molal entropies, since their values will be relative to  $S_1^0|_{T=0}$ , taken as zero, by the third law.

The calculation of  $\bar{S}_2^{\text{cr}}$  as presented here involves a different approach from that used by Hinchey and Cobble (1970), and so a direct comparison of the values obtained in each case is not very meaningful. The latter authors estimated the entropies of the crystals, primarily from the heat

capacity measurements of Hellwege et al. (1961) and of Pfeffer (1961a, 1961b, and 1962). These measurements have been shown to be in error by as much as 2%, due to occluded water. The estimated entropies differ from the present values by as much as 3 or 4% as in the case of the Gd salt. Hinchey and Cobble did not have the presently available solution calorimetry results and so they approached the problem of calculating  $\bar{S}_2^0$  via the calculation of the standard state free energy change for the process represented by equation 12, i.e., by means of the solubility product.

## VI. BIBLIOGRAPHY

- Arrhenius, S. (1887), *Z. Physik Chem.* 1, 631.
- Ashworth, T. and Steeple, H. (1968), *Cryogenics* 8, 225.
- Atkinson, G. (1956), The compressibilities of some rare earth nitrates and chlorides in aqueous solution. Unpublished Ph.D. thesis. Ames, Iowa, Library, Iowa State University of Science and Technology.
- Belskii, N. K. and Struchkov, Yu. T. (1965), *Soviet Physics-Crystallography* 10 (1), 15.
- Berry, R. J. (1963), *Can. J. Phys.* 41, 946.
- Betts, R. H. and Dahlinger, O. F. (1959), *Can. J. Chem.* 37, 91.
- Bisbee, W. R. (1960), Some calorimetric studies of the metals and chlorides of Thulium and Lutetium. Unpublished M.S. thesis. Ames, Iowa, Library, Iowa State University of Science and Technology.
- Bommer, H. and Hohmann, E. (1941), *Z. Anorg. Allg. Chem.* 243, 357.
- Brady, G. W. (1960), *J. Chem. Phys.* 33, 1079.
- Clay, R. M. and Staveley, L. A. K. (1966), *Trans. Faraday Soc.* 62, 3065.
- Csejka, D. A. (1961), Some thermodynamic properties of aqueous rare earth chloride solutions. Unpublished Ph.D. thesis. Ames, Iowa, Library, Iowa State University of Science and Technology.
- Debye, P. and Hückel, E. (1923a), *Physik Z.* 24, 185. Original not available; cited in Onsager, L. and Fuoss, R. M. (1932), *J. Phys. Chem.* 36, 2689.
- Debye, P. and Hückel, E. (1923b), *Physik Z.* 24, 305. Original not available; cited in Onsager, L. and Fuoss, R. M. (1932), *J. Phys. Chem.* 36, 2689.
- DeKock, C. W. (1965), Heats of dilution of some aqueous rare earth chloride solutions at 25°C. Unpublished Ph.D. thesis. Ames, Iowa, Library, Iowa State University of Science and Technology.
- Dieke, G. H. (1968), *Spectra and Energy Levels of Rare Earth Ions in Crystals*, New York, N.Y., Interscience Publishers.
- Duffy, W. T., Lubbers, J., Van Kempen, H., Haseda, T., and Miedema, A. R. (1963), Antiferromagnetic spin ordering below 1°K, in *Proceedings of the 8th International Conference on Low Temperature Physics*, Davies, R. O., Ed., Washington, D.C., Butterworths.

- Dye, J. L. and Spedding, F. H. (1954), *J. Amer. Chem. Soc.* 76, 888.
- Edelin De la Praudiere, P. L. and Staveley, L. A. K. (1964), *J. Inorg. Nucl. Chem.* 26, 1713.
- Gaede, W. (1902), *Physik Z.* 4, 105. Original not available; cited in Westrum, E. F., Furukawa, G. T., and McCullough, J. P. (1968), *Adiabatic low-temperature calorimetry*, in *Experimental Thermodynamics*, McCullough, J. A. and Scott, D. T., Eds., New York, N.Y., Plenum Press, Vol. 1, p. 133.
- Gehring, F. D. and Gerstein, B. C. (1967), *Rev. Sci. Instrum.* 38, 280.
- Gerstein, B. C. (1960), *Heat capacity and magnetic susceptibility of Thulium Ethylsulfate*. Unpublished Ph.D. thesis. Ames, Iowa, Library, Iowa State University of Science and Technology.
- Gildseth, W. M. (1964), *Volume-temperature relationships of some rare-earth chloride solutions*. Unpublished Ph.D. thesis. Ames, Iowa, Library, Iowa State University of Science and Technology.
- Ginnings, D. C. and Furukawa, G. T. (1953), *J. Amer. Chem. Soc.* 72, 522.
- Gopal, E. S. R. (1966), *Specific Heats at Low Temperatures*, New York, N.Y., Plenum Press.
- Graeber, E. J., Conrad, G. H., and Dulier, S. F. (1966), *Acta Crystallogr.* 21, 1012.
- Grenthe, I. (1964), *Acta Chem. Scand.* 18, 293.
- Haeseler, G. and Matthes, F. (1965), *J. Less-Common Metals* 9, 133.
- Hall, R. E. and Harkins, W. D. (1916), *J. Amer. Chem. Soc.* 38, 2658.
- Hansen, M. (1958), *Constitution of Binary Alloys*, New York, N.Y., McGraw-Hill, p. 303.
- Harned, H. S. and Owen, B. B. (1943), *The Physical Chemistry of Electrolytic Solutions*, 1st ed, New York, N.Y., Reinhold Publishing Corporation.
- Heiser, D. J. (1958), *A study of thermodynamic properties of electrolytic solutions of rare earths*. Unpublished Ph.D. thesis. Ames, Iowa, Library, Iowa State University of Science and Technology.
- Hellwege, K. H., Johnson, U., and Pfeffer, W. (1959), *Z. Phys.* 154, 301.
- Hellwege, K. H., Küch, F., Niemann, K., and Pfeffer, W. (1961), *Z. Phys.* 162, 358.
- Hellwege, K. H., Pfeffer, W., and Thiel, H. J. (1962), *Z. Phys.* 168, 474.

- Hinchey, R. J. and Cobble, J. W. (1970), *Inorg. Chem.* 9 (4), 917.
- Jekel, E. C., Criss, C. M., and Cobble, J. W. (1964), *J. Amer. Chem. Soc.* 86, 5404.
- Jenkins, I. L. and Monk, C. B. (1950), *J. Amer. Chem. Soc.* 72, 2695.
- Jones, G. and Bickford, C. F. (1934), *J. Amer. Chem. Soc.* 56, 602.
- Kahle, H. G. (1956), *Z. Phys.* 145, 347.
- Kolthoff, I. M. and Sandell, E. B. (1952), *Textbook of Quantitative Inorganic Analysis*, 3rd ed, New York, N.Y., The Macmillan Company.
- Krumholz, P. (1964), *Solution chemistry, in Progress in the Science and Technology of Rare Earths*, Eyring, L., Ed., New York, N.Y., The Macmillan Company, Vol. 1, p. 110.
- La Mer, V. K. and Goldman, F. H. (1929), *J. Amer. Chem. Soc.* 51, 2632.
- Lange, E. and Niederer, W. (1955), *Z. Electrochem.* 60, 362.
- Latimer, W. M. (1951), *J. Amer. Chem. Soc.* 73, 1480.
- Levy, P. M. (1964), *J. Phys. Chem. Solids* 25, 431.
- Lewis, G. N. (1901), *Proc. Amer. Acad. Arts Sci.* 37, 49.
- Lewis, G. N. (1907), *Proc. Amer. Acad. Arts Sci.* 43, 259.
- Lewis, G. N. and Randall, M. (1961), *Thermodynamics*, revised by Pitzer, K. S. and Brewer, L., New York, N.Y., McGraw-Hill.
- Lohr, H. R. and Cunningham, B. B. (1951), *J. Amer. Chem. Soc.* 73, 2025.
- Longworth, L. G. and MacInnes, D. A. (1938), *J. Amer. Chem. Soc.* 60, 3070.
- Mackay, J. L., Powell, J. E., and Spedding, F. H. (1962), *J. Amer. Chem. Soc.* 84, 2047.
- Marezio, M., Plettinger, H. A., and Zachariasen, W. H. (1961), *Acta Crystallogr.* 14, 234.
- Mason, C. N. (1938), *J. Amer. Chem. Soc.* 60, 1638.
- Mason, C. M. (1941), *J. Amer. Chem. Soc.* 63, 220.
- Matignon, C. (1906a), *Ann. Chim. Phys., Series 8*, 8, 402.
- Matignon, C. (1906b), *Ann. Chim. Phys., Series 8*, 8, 426.

- Milner, S. R. (1912), *Phil. Mag.*, Series 6, 23, 551.
- Milner, S. R. (1913), *Phil. Mag.*, Series 6, 25, 742.
- Moeller, T., Birnbaum, E. R., Forsberg, J. H., and Gayhart, R. B. (1968), Some aspects of the co-ordination chemistry of the rare earth metal ions, in *Progress in the Science and Technology of the Rare Earths*, Eyring, L., Ed., New York, N.Y., Pergamon Press, Vol. 3, p. 61.
- Nathan, C. C., Wallace, W. E., and Robinson, A. L. (1943), *J. Amer. Chem. Soc.* 65, 790.
- Nelson, R. A. (1960), Some thermodynamic properties of aqueous solutions of Terbium. Unpublished M.S. thesis. Ames, Iowa, Library, Iowa State University of Science and Technology.
- Nernst, W. (1910), *Sitz. kgl. preuss. Akad. Wiss.* 12, (13), 261. Original not available; cited in *Chem. Abstr.* (1910), 4, 2397.
- Noyes, A. A. (1924), *J. Amer. Chem. Soc.* 46, 1080.
- Noyes, A. A. and Johnson, J. (1909), *J. Amer. Chem. Soc.* 31, 987.
- Onsager, L. (1927), *Physik Z.* 28, 227. Original not available; cited in Harned, H. S. and Owen, B. B., *The Physical Chemistry of Electrolytic Solutions*, 1st ed, New York, N.Y., Reinhold Publishing Corporation.
- Onsager, L. and Fuoss, R. M. (1932), *J. Phys. Chem.* 36, 2689.
- Pepple, G. W. (1967), Relative apparent molal heat contents of some aqueous rare-earth chloride solutions at 25°C. Unpublished Ph.D. thesis. Ames, Iowa, Library, Iowa State University of Science and Technology.
- Petheram, H. H. (1963), Osmotic and activity coefficients of some aqueous rare-earth chloride solutions at 25°C. Unpublished M.S. thesis. Ames, Iowa, Library, Iowa State University of Science and Technology.
- Pfeffer, W. (1961a), *Z. Phys.* 162, 413.
- Pfeffer, W. (1961b), *Z. Phys.* 164, 295.
- Pfeffer, W. (1962), *Z. Phys.* 168, 305.
- Robinson, R. A. (1937), *J. Amer. Chem. Soc.* 59, 84.
- Robinson, R. A. (1939), *Trans. Faraday Soc.* 35, 1229.
- Robinson, R. A. and Stokes, R. H. (1955), *Electrolyte Solutions*, New York, N.Y., Academic Press Incorporated.



- Saeger, V. W. (1960), Some physical properties of rare-earth chlorides in aqueous solution. Unpublished Ph.D. thesis. Ames, Iowa, Library, Iowa State University of Science and Technology.
- Shedlovsky, T. (1950), J. Amer. Chem. Soc. 72, 3680.
- Shedlovsky, T. and MacInnes, D. A. (1939), J. Amer. Chem. Soc. 61, 200.
- Sieverts, A. and Gotta, A. (1928), Anorg. Allg. Chem. 172, 1.
- Skochdopole, R. E. (1954), Low temperature heat capacities of Thorium, Gadolinium and Erbium. Unpublished Ph.D. thesis. Ames, Iowa, Library, Iowa State University of Science and Technology.
- Spedding, F. H. and Atkinson, G. (1959), Properties of rare earth salts in electrolytic solutions, in The Structure of Electrolytic Solutions, Hamer, W. J., Ed., New York, N.Y., John Wiley and Sons Incorporated, p. 319.
- Spedding, F. H., Csejka, D. A., and DeKock, C. W. (1966), J. Phys. Chem. 70, 2423.
- Spedding, F. H. and Daane, A. H., Eds. (1961), The Rare Earths, New York, N.Y., John Wiley and Sons Incorporated.
- Spedding, F. H. and Dye, J. L. (1954), J. Amer. Chem. Soc. 76, 879.
- Spedding, F. H. and Flynn, J. P. (1954a), J. Amer. Chem. Soc. 76, 1474.
- Spedding, F. H. and Flynn, J. P. (1954b), J. Amer. Chem. Soc. 76, 1477.
- Spedding, F. H. and Jaffe, S. (1954a), J. Amer. Chem. Soc. 76, 382.
- Spedding, F. H. and Jaffe, S. (1954b), J. Amer. Chem. Soc. 76, 384.
- Spedding, F. H. and Jones, K. C. (1966), J. Phys. Chem. 70, 2450.
- Spedding, F. H. and Miller, C. F. (1952a), J. Amer. Chem. Soc. 74, 3158.
- Spedding, F. H. and Miller, C. F. (1952b), J. Amer. Chem. Soc. 74, 4195.
- Spedding, F. H., Naumann, A. W., and Eberts, R. E. (1959), J. Amer. Chem. Soc. 81, 23.
- Spedding, F. H. and Pikal, M. J. (1966), J. Phys. Chem. 70, 2430.
- Spedding, F. H., Pikal, M. J., and Ayers, B. O. (1966), J. Phys. Chem. 70, 2440.
- Spedding, F. H., Porter, P. E., and Wright, J. M. (1952a), J. Amer. Chem. Soc. 74, 2055.

- Spedding, F. H., Porter, P. E., and Wright, J. M. (1952b), J. Amer. Chem. Soc. 74, 2778.
- Spedding, F. H., Porter, P. E., and Wright, J. M. (1952c), J. Amer. Chem. Soc. 74, 2781.
- Spedding, F. H. and Yaffe, I. S. (1952), J. Amer. Chem. Soc. 74, 4751.
- Walters, J. P. (1968), Partial molar heat capacities of some aqueous rare earth chlorides, nitrates, and perchlorates from tenth molal to saturation at 25°C. Unpublished Ph.D. thesis. Ames, Iowa, Library, Iowa State University of Science and Technology.
- Westrum, E. F., Chien Chou, Osborne, D. W., and Flotow, H. E. (1967), Cryogenics 7 (1), 43.
- Westrum, E. F., Furukawa, G. T., and McCullough, J. P. (1968), Adiabatic low-temperature calorimetry, in Experimental Thermodynamics, McCullough, J. P. and Scott, D. T., Eds., New York, N.Y., Plenum Press, Vol. 1, p. 133.
- White, G. K. (1968), Experimental Techniques in Low-Temperature Physics, 2nd ed, London, Oxford University Press.
- White, W. P. (1914a), J. Amer. Chem. Soc. 36, 1856.
- White, W. P. (1914b), J. Amer. Chem. Soc. 36, 1868.

## ACKNOWLEDGEMENTS

The author wishes to express his gratitude to Dr. B. C. Gerstein and to Dr. F. H. Spedding for their suggestions about, guidance of, and continued interest in this work. Thanks are also due: to Dr. H. F. Franzen for some valuable discussions of the interpretation of the results, to the personnel of the groups directed by Dr. V. A. Fassel, Dr. H. J. Svec, and Dr. C. V. Banks for performing the analyses of the samples, and to Mr. C. B. Thaxton for providing the precession photographs of the Lu salt. Most especially is the author in debt to his wife not only for typing the rough draft and checking the bibliography of this thesis, but for her general patience during some trying times.